1985

Vibronic activity probed by laser jet spectroscopy

Jonathan A. Warren
Iowa State University

INFORMATION TO USERS

This reproduction was made from a copy of a manuscript sent to us for publication and microfilming. While the most advanced technology has been used to photograph and reproduce this manuscript, the quality of the reproduction is heavily dependent upon the quality of the material submitted. Pages in any manuscript may have indistinct print. In all cases the best available copy has been filmed.

The following explanation of techniques is provided to help clarify notations which may appear on this reproduction.

1. Manuscripts may not always be complete. When it is not possible to obtain missing pages, a note appears to indicate this.

2. When copyrighted materials are removed from the manuscript, a note appears to indicate this.

3. Oversize materials (maps, drawings, and charts) are photographed by sectioning the original, beginning at the upper left hand corner and continuing from left to right in equal sections with small overlaps. Each oversize page is also filmed as one exposure and is available, for an additional charge, as a standard 35mm slide or in black and white paper format.*

4. Most photographs reproduce acceptably on positive microfilm or microfiche but lack clarity on xerographic copies made from the microfilm. For an additional charge, all photographs are available in black and white standard 35mm slide format.*

***For more information about black and white slides or enlarged paper reproductions, please contact the Dissertations Customer Services Department.**

Warren, Jonathan A.

VIBRONIC ACTIVITY PROBED BY LASER JET SPECTROSCOPY

Iowa State University PH.D. 1985

PLEASE NOTE:

In all cases this material has been filmed in the best possible way from the available copy. Problems encountered with this document have been identified here with a check mark __✓__.

1. Glossy photographs or pages _____
2. Colored illustrations, paper or print _____
3. Photographs with dark background _____
4. Illustrations are poor copy _____
5. Pages with black marks, not original copy _____
6. Print shows through as there is text on both sides of page _____
7. Indistinct, broken or small print on several pages ✓
8. Print exceeds margin requirements _____
9. Tightly bound copy with print lost in spine _____
10. Computer printout pages with indistinct print _____
11. Page(s) _____ lacking when material received, and not available from school or author.
12. Page(s) _____ seem to be missing in numbering only as text follows.
13. Two pages numbered _____. Text follows.
14. Curling and wrinkled pages _____
15. Dissertation contains pages with print at a slant, filmed as received _____
16. Other _____

_____

_____

University
Microfilms
International

Vibronic activity probed by laser jet spectroscopy

by

Jonathan A. Warren

A Dissertation Submitted to the

Graduate Faculty in Partial Fulfillment of the

Requirements for the Degree of

DOCTOR OF PHILOSOPHY

Department: Chemistry
Major: Physical Chemistry

Approved:

Signature was redacted for privacy.

In Charge of Major Work

Signature was redacted for privacy.

For the Major Department

Signature was redacted for privacy.

For the Graduate College

Members of the Committee:

Signature was redacted for privacy.

Iowa State University
Ames, Iowa

1985

TABLE OF CONTENTS

GENERAL INTRODUCTION

The introduction of the technique of laser jet spectroscopy has substantially improved the ability of the molecular spectroscopist to probe fundamental aspects of the optical spectroscopy of polyatomic molecules. Of primary concern to this manuscript is the manifestation of vibronic coupling in absorption and fluorescence. Mechanisms which lead to mirror symmetry breakdown (MSB) by the occurrence of asymmetries in selective absorption and fluorescence transitions are analyzed in an attempt to reveal details of the vibronic activity involved.

In Section I (1), the gross features of the spectra of β-methylnaphthalene are discussed heuristically in terms of excited state mode mixing. While the source of the mode mixing is not readily determinable from the data presented, it is clear that the observed MSB is vibronically induced and the result of either a Duschinsky rotation of excited state normal coordinates or vibronically induced anharmonicity, or both.

In Section II (2), the laser jet spectra of β-methylnaphthalene are reinvestigated with the use of an improved experimental system. The vastly improved resolution and sensitivity of this second system allow for a far more quantitative discussion of the observed excited state mode mixing. From the data obtained from single vibronic level (SVL) fluorescence spectra, it is shown through first order perturbation modeling that the inducing mechanism for MSB in the species is primarily a Duschinsky rotation. The importance of vibronically induced anharmonicity to fourth order is also discussed.

In Section III (3), the vibronic activity in the laser jet spectra of phenanthrene is probed. Transitions involving totally symmetric vibrational modes of the molecule are shown to reveal serious interferences between Condon and Herzberg-Teller induced moments. Model calculations using first order perturbation formulae are performed which accurately reproduce the observed spectra. For transitions involving nontotally symmetric modes, MSB is shown to result from normal coordinate Duschinsky rotation and from Fermi resonance. The inability of known theories to account for the spectra of perdeuterated phenanthrene is also discussed.

An important consideration in using the technique of laser jet spectroscopy to obtain information concerning intramolecular vibronic coupling is whether interferences from impurities in samples of analytes can be avoided. In the Appendix (4), it is shown that such interferences occur only in the event of complexation. Thus, in the absence of such complexation, dispersed fluorescence spectra from SVL spectra are representative of the excited species while excitation spectra of mixtures appear as weighted sums of the spectra of the individual components. It is shown that excitation spectra of mixtures of polycyclic aromatic hydrocarbons can, thus, be used to determine the presence of geometrical isomers in real samples.

EXPERIMENTAL

The experimental scheme which is used to obtain the data presented in this manuscript is based on previous designs of rotationally cooled laser induced fluorescence (RC-LIF) apparatus (5). Since the technique is a simple one which has developed into a rather standard method of obtaining spectral information of cold vaporous species, a detailed description of the technique will not be presented here. Instead, this section is meant to provide the reader with a brief review of the principles behind the technique and details are given only with respect to the apparatus used. Two separate experimental systems were constructed for the experiments described here. The first system will be referred to as the 'continuous' system since the nozzle used in the apparatus was operated in a continuous mode. This system was used for the experiments related in Section I and the Appendix. A second improved system was later developed and used for the experiments discussed in Sections II and III. This system will be referred to as the 'pulsed' system since the nozzle used was synchronously pulsed with the laser.

RC-LIF is based on the merging of two separate techniques: supersonic expansions providing rotationally cooled jets of vaporous materials and laser induced fluorescence spectroscopy. In 1974, the first laser photoexcitation spectrum of NO_2 was observed (6) in a supersonic expansion of argon. The rotational temperature of the NO_2 was determined to be roughly 3 K which produced spectra absent of vibrational and rotational hot bands. The simplified spectra were, therefore, more

amenable to analysis. The later application of the technique to much larger polyatomic species showed that essentially involatile materials could be observed in the gas phase at internal temperatures less than 1 K. Such conditions are ideal for spectroscopic analysis as interferences due to spectral congestion and medium induced effects are absent.

The low internal temperatures are obtained by the expansion of a gas from a high pressure region into a low pressure region through an orifice. As the pressure differential and orifice size are increased, the cooling efficiency is increased. Under typical conditions, a vaporous analyte is diluted to several atmospheres pressure with an inert gas and expanded into a vacuum chamber through a nozzle containing an orifice with a diameter less than 1 mm. As the material passes through the orifice, random translational motion becomes directed into the direction of flow. As a result, the Maxwellian velocity distribution which defines the translational temperature of the fluid narrows. The bulk gas proceeds to equilibrate its internal temperatures with the lowered translational temperature and, thus, attains drastically lowered rotational and vibrational temperatures. As the expansion continues into the vacuum chamber, the density and random thermal motion become sufficiently small that a collisionless regime is reached. At this point, the jet can be probed with an intersecting laser beam and the resulting fluorescence detected perpendicularly to the two beams.

A diagram of this scheme is shown in Fig. 1 of the Appendix. After the laser beam exits the expansion chamber, it is impinged upon a cell containing a solution of fluorescing dye. The resulting fluorescence is

detected and used as a reference for the laser intensity. Laser induced fluorescence from the expanding gas is collected and imaged onto the slits of a detecting monochromator. The intensity of this fluorescence is then measured and normalized to the laser intensity before recording.

The first system constructed for these experiments is based on early designs (5) of continuously flowing expansion apparatus. The nozzle is prepared by rotating the end of a length of glass capillary tubing in an open flame until sealed. After cooling, the tip is ground back until an orifice of 160 ± 10 μm is left. Glass to metal seals provide suitable connections to sample holders and gas cylinders. The nozzle is mounted in a three axis mount onto the vacuum chamber which is constructed from 4 in. stainless steel tubing. Internal chamber pressures are maintained during operation by 4 in. oil diffusion pumps operating at 300 L/s with a 50 L/s mechanical forepump. The low pumping speeds and the fact that the gas flows into the system through the nozzle continuously requires that pressures in the high pressure region of the apparatus be limited to 2 atm. Helium is used as the diluting or carrier gas. Heating of samples to generate high vapor densities of analytes in the high pressure region is obtained by wrapping the sample holder with a coil of heating cord which is controlled by a temperature controller to maintain a constant temperature. In this system, sample temperatures up to 150°C are obtainable.

The probe laser beam is the output from a Quanta-Ray Nd:YAG pumped dye laser. Typically, this beam is frequency doubled by a KDP crystal mounted in an Inrad Autotracker which angle tunes the crystal during

scanning of the laser wavelength. The doubled laser beam is focused with a 50 cm focal length lens into the expansion chamber through light baffles mounted along the laser entrance and exit arms of the chamber. These baffles are fabricated from stainless steel disks, each having a central aperture of 2 to 5 mm, which are placed inside lengths of 0.5 in. stainless steel tubing and painted black. The baffles are used to reduce the amount of scattered laser light detected by the signal photomultiplier tube.

After the laser intercepts the rotationally cooled jet 5 mm (about 30 nozzle diameters) downstream of the orifice and exits the chamber, the laser beam is directed into a cell containing a dilute solution of rhodamine B where the resulting fluorescence is detected with a photomultiplier tube (RCA 1P28). The output from this is sent to a charge sensitive preamplifier and then to the reference channel of a Molectron LP-20 laser photometer.

The laser induced fluorescence from the expanding jet is collected at right angles to both the jet and laser beam by an f/2.5 lens and then focused into a 0.3 meter f/4.2 Instruments SA monochromator. The output from the detection photomultiplier tube (RCA 1P28-A) is then preamplified and sent to the signal channel of the laser photometer. The signals to the laser photometer are then averaged and ratioed and sent to a strip chart recorder to record the normalized spectrum.

The spectra which were obtained from the continuous system described above were adequate for the characterization and analysis of species in mixed samples and the qualitative analysis of vibronic ac-

tivity in β-methylnaphthalene. However, to obtain the detailed spectra required to perform quantitative studies of vibronic coupling, a system was needed which would provide improved cooling, enhanced detection sensitivity, and superior signal to noise ratios. To this end, a second system was constructed which utilized a pulsed nozzle.

The pulsed system is designed after the continuous system, but several modifications in the equipment used are made. The nozzle is a Quanta-Ray PSV-2 pulsed valve fitted with a 0.5 mm orifice. The valve is solenoid actuated and can be operated synchronously with the laser by use of internal triggering. Gas pulses of 60 μsec duration are provided trough the expansion orifice timed appropriately with the probe laser operating at 10 Hz. The drastically reduced load on the vacuum system required to pump away the expanded gas allows for a larger orifice diameter and higher backing pressures than in a continuously flowing system. The result is that a vastly improved cooling efficiency and higher analyte throughputs are obtained.

The pulsed valve is mounted on a three axis mount inside an aluminum walled expansion chamber. Internal chamber pressures of 1-5 x 10^{-5} Torr are maintained during operation by a 1740 L/s 6 in. diffusion pump stack. Backing pressures of the helium carrier gas are limited to 10 atm. Samples of desired analytes are placed inside the heated valve assembly head of the PSV-2. Thermally equilibrated vapor pressures from solid samples at up to 110°C are obtained in this manner.

As with the continuous system, a Quanta-Ray laser is frequency doubled, lightly focused into the expansion chamber and deflected into

a reference cell containing rhodamine B. However, to reduce scattered light further, light baffles are used which are made with polished home-made beam skimmers (7) and Brewster angle windows. This combination produces spectra which are virtually free of scattered light contributions. In addition, to improve fluorescence detection, f/1.0 collection optics are placed inside the expansion chamber. For photoexcitation spectra, a 0.10 meter Instruments SA monochromator is used as the detection spectrophotometer. For dispersed fluorescence spectra, a 0.32 meter instrument is used. When scattered light levels are low, photoexcitation spectra are recorded using the holographic grating of the 0.10 meter monochromator in zero order so that the spectrometer acts only as an attenuator. When higher scattered light levels are encountered, it is used in first order by centering its 160 A bandpass red of the laser wavelength in a spectral region of strong analyte fluorescence.

The detection photomultiplier used in the pulsed system is a Hamamatsu R106-UH. A Quanta-Ray DGA-1 gated amplifier connected to an LSI-11 based computer is used for data analysis and storage. Scanning of both the laser and monochromator wavelengths are computer controlled. For dispersed fluorescence spectra, where a single vibronic level is excited by the probe laser and the resulting fluorescence is dispersed, a spectrum is obtained by collecting data while slewing the monochromator across the region of interest repetitively and simultaneously averaging the data. In this manner, day long scans can be recorded without distortions to the spectra from baseline shifts or long term instrument response changes. Excitation spectra are recorded by scanning the

laser to a specified wavelength and collecting data for a preselected number of laser shots before scanning to the next wavelength. Careful normalization to laser intensity ensures accurate relative intensities in photoexcitation spectra to within 5%. Dispersed fluorescence spectra reveal accurate relative intensities to within the approximation of a flat spectral response of the detection photomultiplier.

For dispersed fluorescence spectra and most photoexcitation spectra, the $<0.4\ cm^{-1}$ FWHM output of the laser is used. To obtain rotationally resolved spectra, the pressure tuned etalon option in the dye laser is utilized to obtain high resolution ($0.05\ cm^{-1}$ FWHM) excitation scans over short regions ($\sim 18\ cm^{-1}$) of the spectrum. The output voltage of a calibrated pressure transducer is then recorded simultaneously with the fluorescence intensity to determine relative band positions and contour widths.

Samples are prepared from naphthalene (Aldrich, 98%), α-methylnaphthalene (Aldrich, 97%), β-methylnaphthalene (Fluka, 97%), β-methylnaphthalene-d_{10} (MSD Isotopes, 99.1%), and phenanthrene-d_{10} (MSD Isotopes, 98.5%) without further purification. Phenanthrene (Fluka, 97%) is used after 80-100 passes through a zone refiner to remove traces of anthracene.

SECTION I. SYMMETRY REDUCTION-VIBRONICALLY INDUCED MODE MIXING IN THE S_1 STATE OF β-METHYLNAPHTHALENE

ABSTRACT

Supersonic jet excitation and single vibronic level (SVL) dispersed fluorescence spectra for α- and β-methylnaphthalene (S_1 state) are presented. Marked mirror symmetry breakdown between the excitation and origin excited fluorescence spectra of the β-isomer is observed. The SVL spectra reveal that mode mixing in the S_1 state is too extensive to be accounted for by first order treatment of the Duschinsky effect. Vibronically induced mode mixing in the β-isomer is suggested as the mechanism which leads to intramolecular vibrational energy redistribution which onsets at a significantly lower excess vibrational energy than in naphthalene. The implications of our findings for other polyatomics are discussed.

INTRODUCTION

Since the late 1960s, the relationship between the vibronic coupling and mirror symmetry breakdown (MSB) associated with $S_1 \rightleftarrows S_0$ absorption and fluorescence spectra of larger polyatomic molecules has received considerable attention (1-12). Of particular interest for this paper are the mechanisms for MSB stemming from adiabatic coupling, i.e., when the electronic energy gaps between S_1 and coupled states S_j are large relative to the vibrational mode frequencies. For this case, intensity MSB can arise for transitions associated with a pure mode when it is both Herzberg-Teller (HT) and Condon allowed (1,2). Certain totally symmetric fundamentals exhibit this behavior in the optical spectra of naphthalene's lowest excited singlet state (3,4). MSB can also arise from the mixing of ground state modes (normal coordinates) in the excited state, the Duschinsky effect (13). The Duschinsky effect or rotation stems from the off-diagonal quadratic terms in the expansion of the S_1 potential energy which utilizes ground state normal coordinates. Mixing is restricted to modes of the same symmetry and is predicted to occur between modes which are Herzberg-Teller active (5,6). This type of mixing has been referred to as medium dependent since electronic energy gaps and, therefore, HT activity are medium dependent. A medium independent Duschinsky mechanism exists as well and appears to be operative in the S_1 states of azulene and certain azaazulenes (7-10).

Early theories established that the effects of Duschinsky mixing on vibronic intensities should be far more pronounced in absorption than

in fluorescence originating from the zero-point level (5,6). Striking examples of this occur for the S_2 state of azulene (7,8) and S_1 states of azaazulenes (9,10) as probed by the mixed crystal technique. For these systems, the absorption spectrum is far more complex than the fluorescence spectrum which is unperturbed and essentially medium independent. For the case of azulene, vibronically induced anharmonicity (cubic) also figures importantly in the absorption structure (7,8).

The above theories also suggest that spectral manifestations of the Duschinsky effect are likely to be more pronounced the lower the point symmetry and the larger the molecule. The investigation of substituted derivatives of aromatic molecules, the parent possessing considerable symmetry and exhibiting HT activity, would appear to be a viable approach to test the former prediction.

To this end, we have investigated the jet cooled fluorescence excitation and dispersed fluorescence spectra associated with the S_1 state of a number of monosubstituted naphthalenes and consider here the results for the α- and β-isomers of methylnaphthalene.

The Herzberg-Teller activity of nontotally symmetric modes in the S_1 state of naphthalene is well characterized (3) and dominated by two b_{1g} fundamentals at 508 and 939 cm^{-1} in the ground state. In the vapor, naphthalene's fluorescence and absorption spectra offer little evidence for mode mixing (14-17). In contrast, β-methylnaphthalene exhibits marked MSB with excitation spectra which are complex and which bear little resemblance to that of the parent. On the other hand, the fluo-

rescence spectra (0_0^0 excitation) of naphthalene and the methylnaphthalenes parallel each other with only minor discernible differences.

Single vibronic level (SVL) dispersed fluorescence spectra are used in conjunction with other data to qualitatively discuss MSB in the methylnaphthalenes in terms of the Duschinsky effect and symmetry reduction. SVL data for the higher excess vibrational energies indicate that intramolecular vibrational energy redistribution via vibronically induced anharmonic interactions onsets at excess energies substantially lower than in naphthalene.

EXPERIMENTAL

The rotationally cooled laser induced fluorescence (RC-LIF) apparatus used has been described elsewhere (18) and will be only briefly discussed here. The output of a Quanta-Ray Nd:YAG pumped dye laser (<0.5 cm^{-1} FWHM) is frequency doubled with a KDP crystal mounted in an Inrad Autotracker and lightly focused through light baffles into the supersonic expansion chamber where it intersects the rotationally cooled jet. The laser beam is exited from the chamber and impinged upon a solution of rhodamine B where the resulting fluorescence is detected with a photomultiplier tube, providing a reference for the laser intensity.

The laser beam intersects the rotationally cooled jet 5-10 mm (30-60 nozzle diameters) downstream of the orifice. The resulting fluorescence propagating perpendicular to the two beams is collected and imaged onto the slits of a 0.32 meter Instruments SA spectrophotometer. The outputs from the signal and reference photomultiplier tubes (both RCA 1P28-A) are then sent to a Quanta-Ray DGA-1 gated amplifier where they are averaged, ratioed, and sent to a strip chart recorder to record the normalized spectrum. Photoexcitation spectra were obtained by opening the monochromator slits to allow a 50 Å bandpass and setting the center wavelength to 3425 Å. Emission of the naphthalenes in this region is relatively weak but unstructured, providing a suitable measure of the relative absorption cross sections of the bands observed in excitation.

The Pyrex nozzle used had a 160 ± 10 μm diameter orifice and was operated in a continuous mode. Samples were prepared from naphthalene (Aldrich 98%), α-methylnaphthalene (Aldrich, 97%), and β-methylnaphthalene (Fluka, 97%) without further purification. We have previously reported the degree of cross contamination in these samples as determined by RC-LIF/GC (19). The room temperature vapor pressures of the samples were diluted with He, maintaining a constant total pressure of 1.0 to 2.0 atm. Under these conditions, internal pressures are maintained at 0.1-0.5 mtorr.

RESULTS AND DISCUSSION

A portion of the photoexcitation spectra of naphthalene, α-, and β-methylnaphthalene in the region of their S_1 origins are shown in Fig. 1. The frequencies of bands are shown relative to the origins at 32,019, 31,773 and 31,705 cm^{-1} for naphthalene and the α- and β-isomers, respectively. Relative intensities of bands with absolute frequencies <32,900 cm^{-1} are accurate as shown but the necessity of a dye change near this frequency means that the relative intensities of bands shown on opposite sides of this frequency are approximate. Nevertheless, the intensities as shown are independent of sample temperatures and jet conditions, indicating that none are impurity bands, bands due to van der Waals complexes or hot bands. Only under very warm jet temperatures do weak features appear which could be assigned as hot bands. All of the bands have laser limited linewidths.

The enhancement in the intensity of the origin band relative to other bands produced by methyl substitution should be noted. This is likely a reasonable measure of the relative importance of Condon and Herzberg-Teller contributions in the three molecules. Given that the Condon transition dipole for the $^1B_{3u}$ state of naphthalene is small due to a rather complete destructive interference between two single electron excited state configurations, a strong dependence of the origin intensity on substitution is expected.

Figure 1 shows that the complexity in vibronic structure increases as one proceeds from naphthalene to β-methylnaphthalene. This is par-

Figure 1. RC-LIF excitation spectra of naphthalene, α(1)-methylnaphthalene, and β(2)-methylnaphthalene. The abscissa indicates band positions relative to the S_1 origins of each of the species. Assignments are provided for several major features in the naphthalene spectrum. Relative intensities of bands separated by several hundred cm^{-1} are only approximate. The intensity of the 0_0^0 band of the β isomer has been reduced by 50%

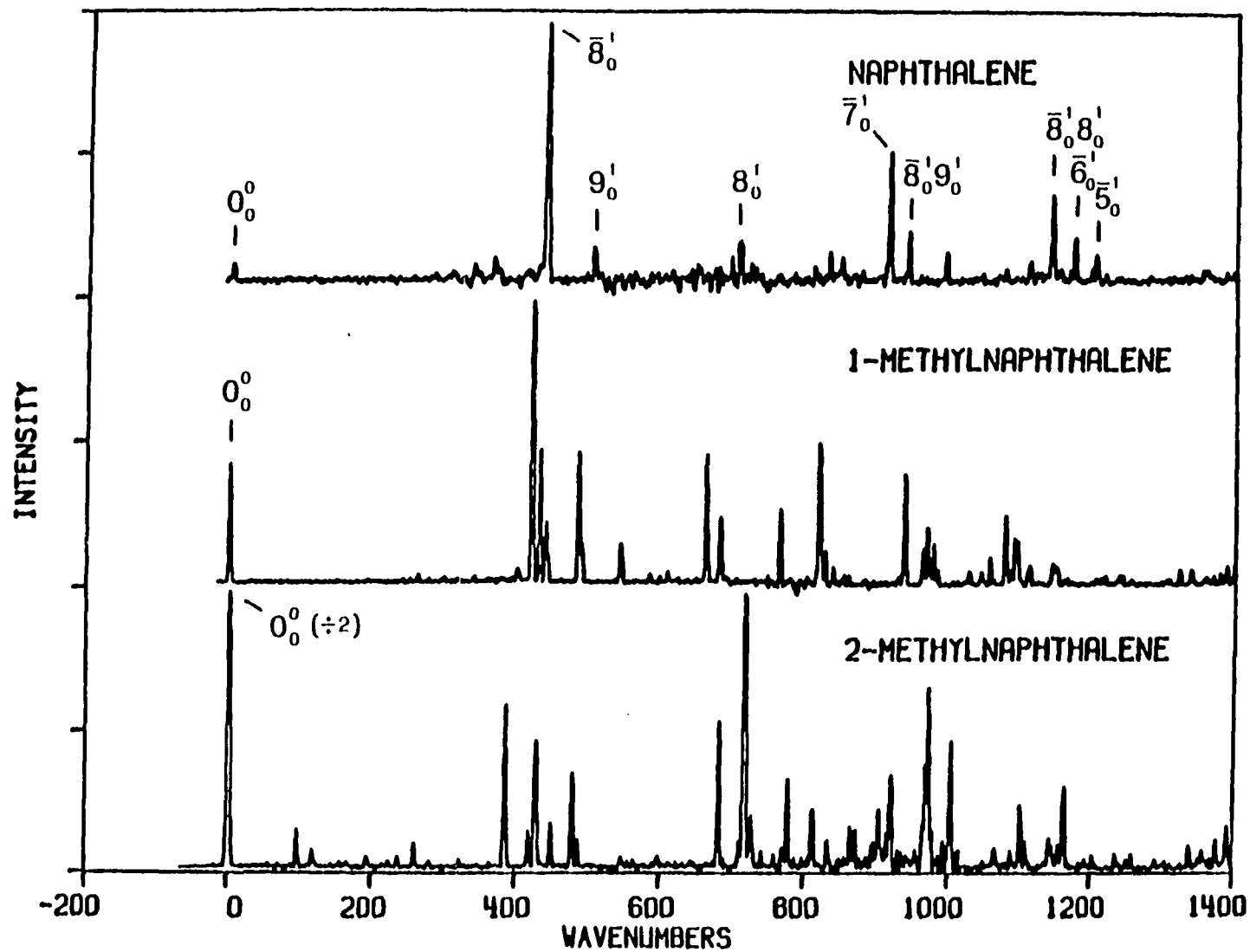
NAPHTHALENE
1-METHYLNAPHTHALENE
2-METHYLNAPHTHALENE
0_0^0
$\bar{8}_0'$
$9_0'$
$8_0'$
$\bar{7}_0'$
$\bar{8}_0'9_0'$
$\bar{8}_0'8_0'$
$\bar{6}_0'$
$\bar{5}_0'$
0_0^0 (÷2)
INTENSITY
-200
0
200
400
600
800
1000
1200
1400
WAVENUMBERS

ticularly evident in the 300-600 cm^{-1} region where for naphthalene, the b_{1g} Herzberg-Teller origin band $\bar{8}_0^1$ at 435 cm^{-1} is dominant. In α-methylnaphthalene, this band remains prominent with a minor frequency shift to 419 cm^{-1} while several additional features appear in the region. In the case of the β-isomer, no feature readily assignable to the $\bar{8}_0^1$ naphthalenic mode is present. Indeed, the excitation spectrum of β-methylnaphthalene bears little resemblance to that of naphthalene. This is in striking contrast to the strong similarities between the origin excited dispersed fluorescence spectra of these species.

Figure 2 shows the fluorescence spectrum obtained by 0_0^0 excitation of β-methylnaphthalene. Aside from the greatly enhanced origin and 5_1^0 features, the spectrum appears largely indistinguishable from that of naphthalene (14). Frequency shifts and relative intensity changes from those of naphthalene of the other major bands are almost immeasurable while only a few new very weak features appear in the spectrum. The spectrum of α-methylnaphthalene shows more substantial shifts in band positions but, nevertheless, appears much like that of naphthalene with only slightly intensified 0_0^0 and 5_1^0 bands.

Clearly, the MSB present in the $S_1 \rightleftarrows S_0$ spectra of naphthalene is the most pronounced for β-methylation. Furthermore, the MSB must be linked to the reduction in symmetry to C_s under which all planar modes (including b_{1g}) are Condon allowed and potentially Herzberg-Teller active. It is highly unlikely, however, that the MSB is due to interference effects between the Condon and HT components of individual vibronic transitions (1-4) since the relaxed fluorescence spectra of naphthalene

Figure 2. RC-LIF dispersed fluorescence spectrum of β-methylnaphthalene obtained by 0_0^0 excitation. The intensity of the resonance fluorescence band has been reduced by 50% after the scattered laser light contribution was subtracted out. Several of the more prominent bands are assigned in terms of naphthalene modes

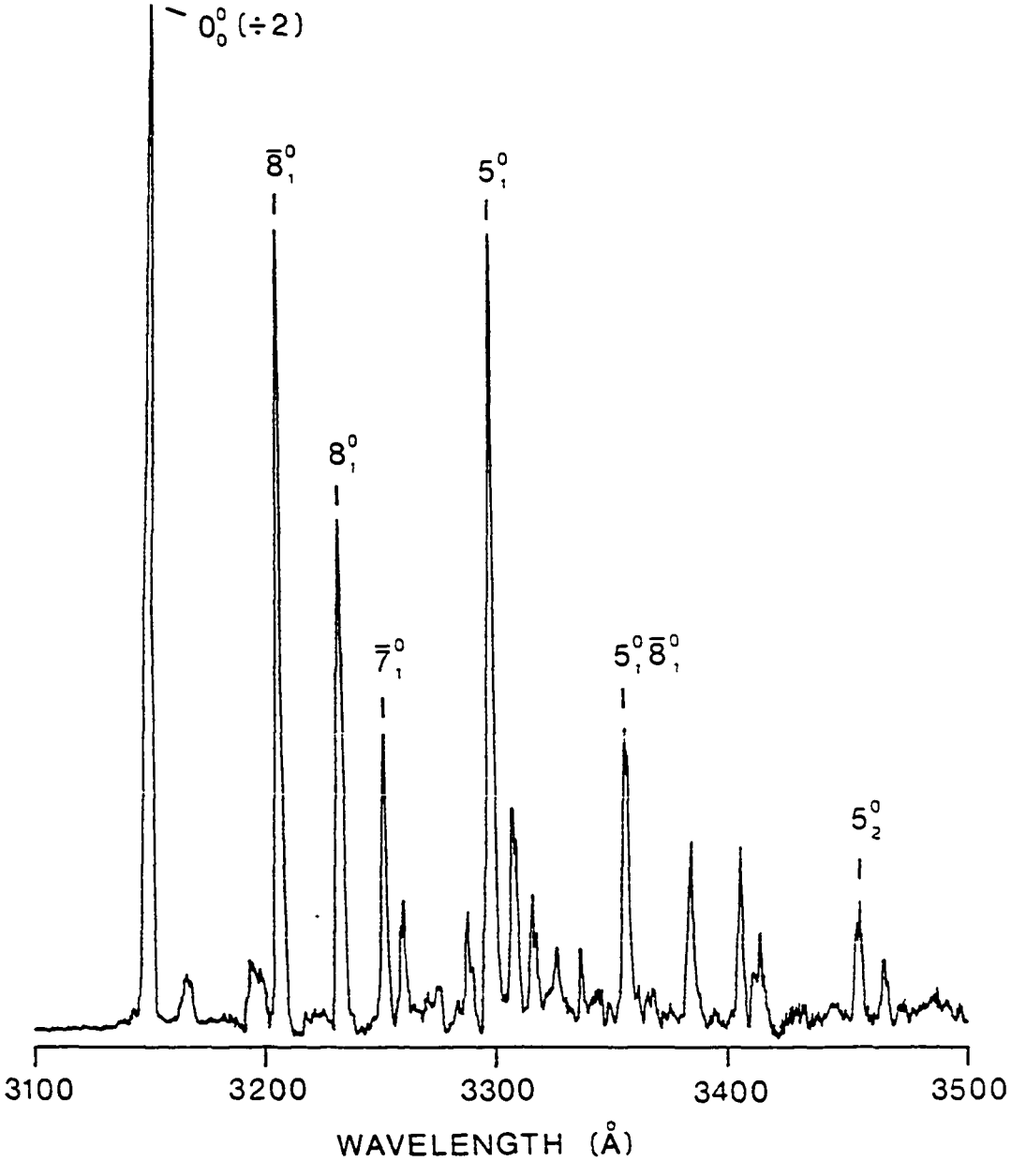
0_0^0 (÷2)
$\bar{8}_1^0$
5_1^0
8_1^0
$\bar{7}_1^0$
$5_1^0\bar{8}_1^0$
5_2^0
3100
3200
3300
3400
3500
WAVELENGTH (Å)

and the methyl isomers are virtually identical. Nor can it be ascribed to an enhancement of intrastate anharmonicity due to symmetry reduction, i.e., anharmonic terms which are not triggered by vibronic coupling between the S_1 and higher energy states. This follows since the relaxed fluorescence and Raman spectra reveal little in the way of anharmonic perturbations.

The most plausible explanation for the MSB is mode mixing in the S_1 state resulting from the Duschinsky effect and, possibly, also vibronically induced anharmonicity. With regard to the former, the absence of a strong $\bar{8}_0^1$ feature in absorption for the β-isomer can be qualitatively understood (5,6) to be a result of mixing between $\bar{8}$ and other modes of the same symmetry (under C_s) which carry relatively little (but some) intrinsic HT intensity. The limit on "little" is set by their apparent absence in fluorescence originating from zero-point. SVL dispersed fluorescence spectra are invaluable for probing the extent of mode mixing. In the 300-600 cm^{-1} region of the excitation spectrum of the β-isomer, only six well isolated features at 385, 417, 427, 450, 478 and 485 cm^{-1} appear with intensities $\gtrsim$1% of the 0_0^0 band. For the SVL data which follows, we note that mixed mode behavior of the pumped level manifests itself as multiplet structure in the 1-1 type fluorescence bands. These effects can be quite dramatic as evidenced in the recent $S_2 \rightarrow S_0$ jet spectra of azulene (20).

Figure 3 shows portions of the dispersed fluorescence spectra obtained pumping two of the stronger features at 427 and 478 cm^{-1} and a weaker feature at 485 cm^{-1}. Each spectrum shows, in addition to a

Figure 3. RC-LIF dispersed fluorescence spectra of β-methylnaphthalene obtained by excitation of (a) 427 cm^{-1}, (b) 478 cm^{-1}, and (c) 485 cm^{-1} S_1 levels. The 1-0 (resonance fluorescence) bands (marked with asterisks) contain large contributions from scattered laser light. Labeled 1-1 bands correspond to ground state levels at (1) 408, (2) 448, (3) 517, (4) 552, and (5) 580 cm^{-1}. Fluorescence bands to the $\overline{8}$ combinations with these levels appear in each spectrum between ~3200 and 3220 A. Instrument resolution is 2.5 A

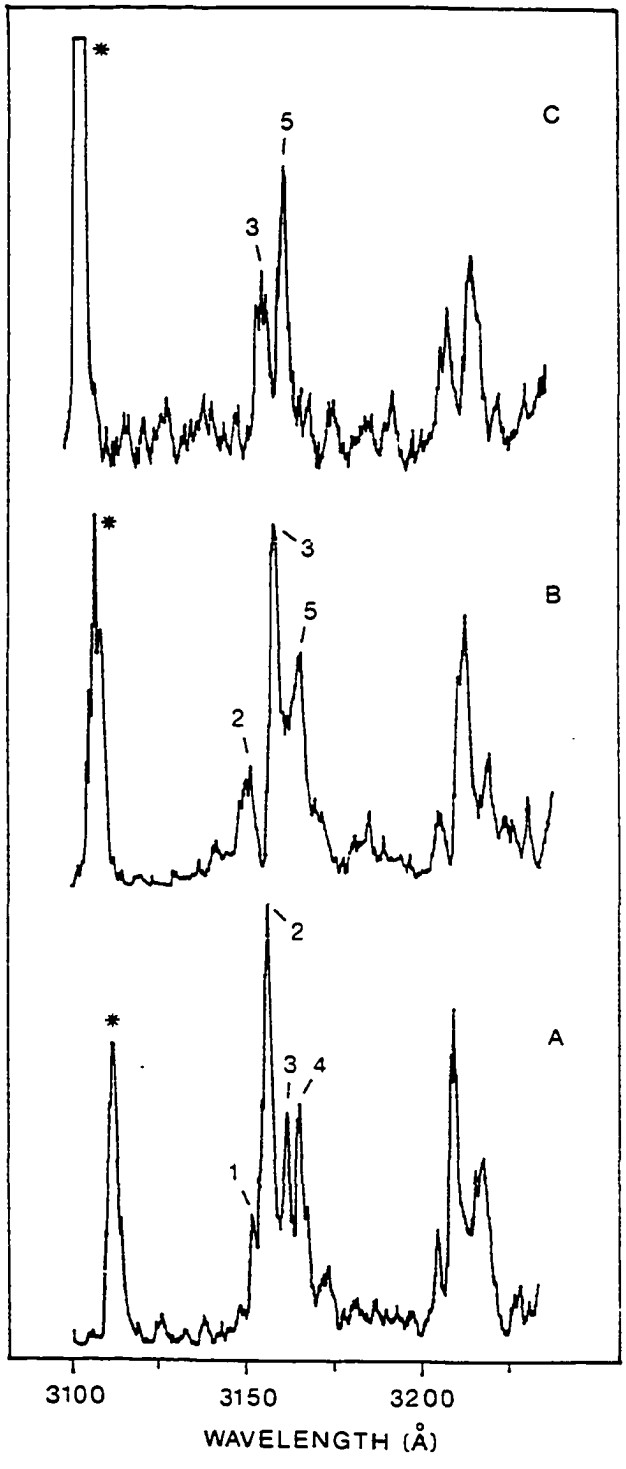
*
5
C
3
*
3
5
B
2
*
2
3
4
A
1
3100
3150
3200
WAVELENGTH (Å)

strong resonance fluorescence band, a multiplet structure in the 1-1 fluorescence region. The remaining portion of each spectrum consists of combination bands of these latter levels with those which are prominent in the origin excited spectrum ($\overline{8}$, 8, $\overline{7}$, 7, 5, etc.) each showing the multiplet structure. The bands corresponding to the $\overline{8}$ additions to the 1-1 bands are shown in Fig. 3. The SVL spectra of the other S_1 levels in the region show similar behavior. At higher resolution, analysis of these six SVL spectra confirms that six ground state modes (at 408, 448, 481, 517, 552 and 580 cm^{-1}) are involved in a conspicuous excited state mode mixing. Each spectrum shows between two and five features comprising the multiplets with one component corresponding to the 517 cm^{-1} $\overline{8}_1$ level appearing in each. The appearance of fluorescence to $\overline{8}_2$ in each of the spectra is decisive since one should not observe fluorescence to this level in the absence of mode mixing unless the level pumped contains $\overline{8}^1$. Though the 417 and 478 cm^{-1} S_1 levels possess the greatest $\overline{8}$ character, it is clear that the other four levels are also endowed.

Within the framework of the first order perturbation theory of the Duschinsky effect, we have been able, with reasonable assigned values of HT coupling matrix elements for the six modes including B, to <u>qualitatively</u> understand the intensities of the six bands in absorption together with the absence of all but $\overline{8}_1^0$ in the origin excited fluorescence. However, we view this as an exercise with little value since this theory predicts that in the 1-1 region of the SVL fluorescence, the multiplet structure should consist of only two bands, corresponding to

transitions terminating at $\overline{8}$ and X in the ground state. The mode X is the one assumed to be weakly HT active (because of symmetry reduction) and mixed with $\overline{8}$ (the intensity source) in the S_1 state. The SVL data show that mode mixing in this state is operative between different X-type modes.

For α-methylnaphthalene, excitation of the strong 419 cm^{-1} band results in fluorescence very similar to that observed for $\overline{8}_0^1$ excitation of naphthalene showing no mixed-mode character. Most of the fluorescence intensity is carried in bands assignable to $\overline{8}_0^1$, $\overline{8}_2^1$, $\overline{8}_0^1 5_1^0$, and $\overline{8}_2^1 5_1^0$. The Condon allowed $\overline{8}_1^1$ and associated features are predictably weak. The appearance of these rather intense features in the β-isomer is clearly a consequence of its enhanced Condon transition dipole, Fig. 1.

This enhancement of the α-relative to the α-isomer can be understood in terms of the one-electron transition density for the S_1 and S_0 states. For naphthalene, simple molecular orbital models with first order configuration would imply that this density is far more sensitive to β-substitution than for α-substitution. This sensitivity may be similarly revealed in the vibronic coupling matrix elements which give rise to Duschinsky rotation.

The behavior observed in the SVL spectra shown in Fig. 3 is not constant for other S_1 levels pumped in β-methylnaphthalene. The dispersed fluorescence spectra of the 100 and 123 cm^{-1} features indicate no mode mixing but rather simple fluorescence showing 1-1 type bands to ground state levels at 155 and 177 cm^{-1}, respectively. It is tempting to assign these to the $4(b_{1u})$ and $4(a_u)$ modes at 166 and 181 cm^{-1} in

naphthalene, but we can provide no suitable explanation for the activity of these out-of-plane modes. The Raman spectrum of β-methylnaphthalene reveals bands at 148 and 171 cm^{-1} (21). Alternatively, these features may be overtones of the strongly anharmonic torsional mode of the methyl substituent. The absence of similar low-frequency structure in combination with other intense features in excitation precludes this assignment. The veritable dearth of reliable information on the vibrational structure of the methylnaphthalenes prevents us from making any further comments concerning the assignments of features observed in the SVL spectra or their counterparts in excitation.

In contrast to the appearance of SVL spectra of low-level S_1 bands, bands to higher energy show increasingly complicated fluorescence structure. Beginning with the 906 cm^{-1} feature, narrowline fluorescence bands can no longer be disentangled from the spectra. Instead, the spectra are dominated by broad (~200-300 cm^{-1} FWHM) features on top of a developing background intensity. Figure 4 shows a typical spectrum obtained by excitation of the 1437 cm^{-1} S_1 feature of β-methylnaphthalene. By ~1600 cm^{-1} in the excited state, S_1 fluorescence is dominated by the unstructured background evident in Fig. 4 which is probably a result of rapid intramolecular vibrational energy redistribution (IVER). The onset of irreversible IVER at ~1600 cm^{-1} is well below that observed for naphthalene (~2500 cm^{-1}). Below 1600 cm^{-1}, the broadened fluorescence bands are more likely due to spectral congestion from advanced mode mixing and level scrambling. Below ~900 cm^{-1}, this congestion is resolvable.

Figure 4. Same as in Fig. 3. Level pumped is 1437 cm^{-1} above S_1 origin of β-methylnaphthalene

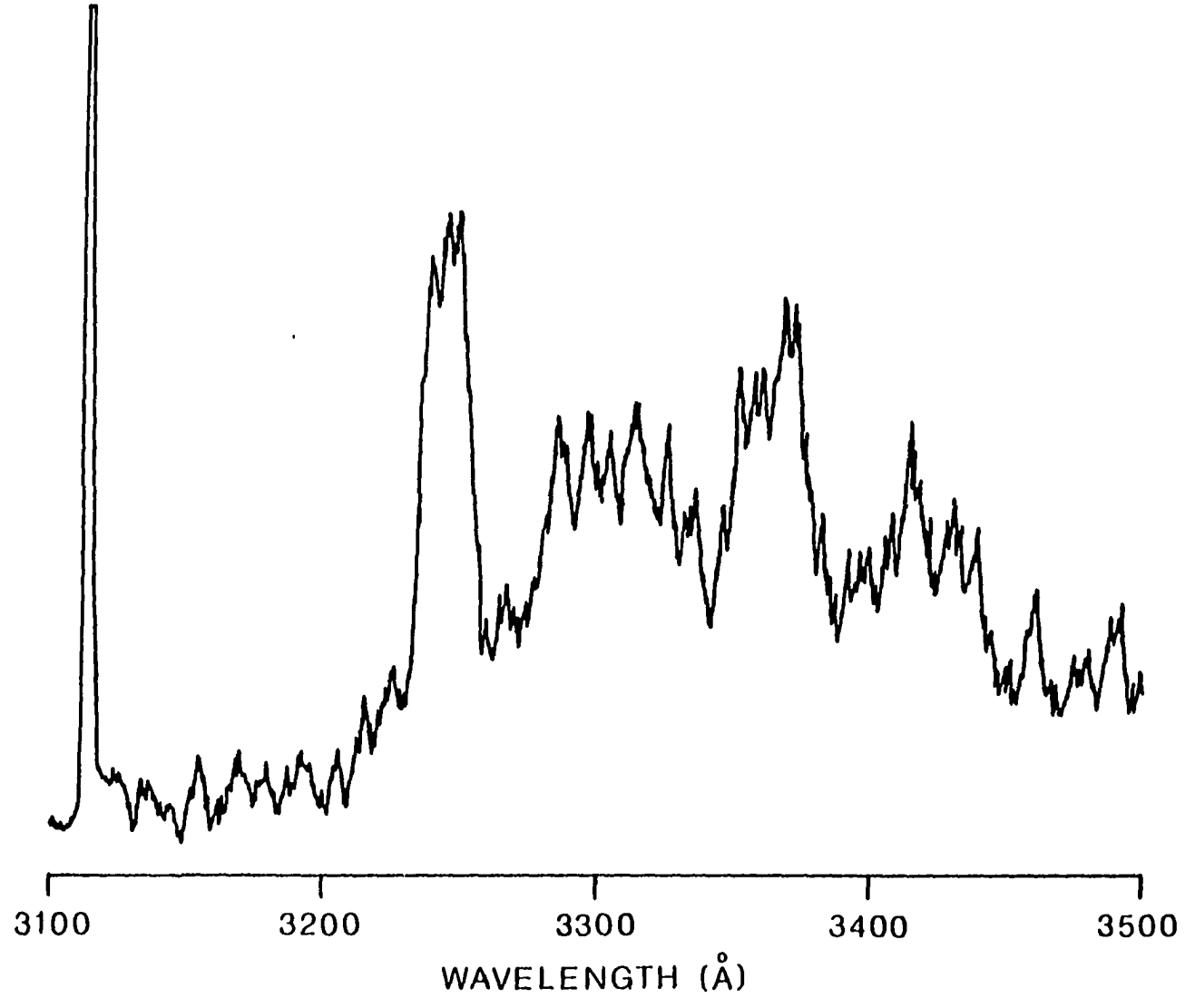
3100
3200
3300
3400
3500
WAVELENGTH (Å)

CONCLUSIONS

Although the mode mixing involving $\overline{8}$ in the S_1 state of β-methylnaphthalene is too strong to be accounted for by the first order perturbation treatment of the Duschinsky effect, the data argue strongly that it is a consequence of symmetry reduction and vibronic coupling. The fact that the mixing in the β-isomer is more severe than in the α-isomer may be explicable in terms of naphthalene's one-electron transition density between the S_1 state and the S_2 state (to which it is dominantly coupled). At the α-position, this density is very small relative to its value at the β-position. For the β-isomer, the possibility that vibronically induced anharmonicity is, in part, responsible for mode mixing in the 300-600 cm^{-1} region cannot be excluded. We suggest that the onset of IVER in β-methylnaphthalene at substantially lower excess vibrational energy than in naphthalene is a consequence of symmetry reduction and this type of anharmonicity. Again, such anharmonicity has been convincingly accounted for in the S_2 state of azulene (7,8).

To what extent do our findings for β-methylnaphthalene carry implications for other molecules? We suggest that it may be considerable for appropriate substitution in molecules which like naphthalene possess an S_1 state which is vibronically coupled to close lying higher energy states, e.g., pyrene and phenanthrene. Vibronically induced mode mixing opens up the possibility that IVER in the excited electronic states of polyatomic molecules will generally be more extensive than in the ground state.

REFERENCES

1. D. P. Craig and G. J. Small, J. Chem. Phys. 50 (1969) 3827.
2. G. R. Hunt and I. G. Ross, J. Mol. Spectrosc. 9 (1962) 50.
3. J. Wesell, Ph.D. Thesis, University of Chicago, Chicago, Illinois, 1970.
4. M. J. Robey, I. G. Ross, R. V. Southwood-Jones, and S. J. Strickler, Chem. Phys. 23 (1977) 207.
5. G. J. Small, J. Chem. Phys. 54 (1971) 3300.
6. B. Sharf and B. Honig, Chem. Phys. Lett. 7 (1970) 132.
7. A. R. Lacey, Ph.D. Thesis, University of Sydney, Sydney, Australia, 1972.
8. A. R. Lacey, E. F. McCoy, and I. G. Ross, Chem. Phys. Lett. 21 (1973) 233.
9. F. B. Burke, D. R. Eslinger, and G. J. Small, J. Chem. Phys. 63 (1975) 1309.
10. G. J. Small and F. P. Burke, J. Chem. Phys. 66 (1977) 1767.
11. G. Orr and G. J. Small, Chem. Phys. Lett. 21 (1973) 395.
12. G. Orr and G. J. Small, Chem. Phys. 2 (1973) 60.
13. F. Duschinsky, Acta Physiochim. 7 (1937) 551.
14. M. Stockburger, H. Gattermann, and W. Klusmann, J. Chem. Phys. 63 (1975) 4519.
15. S. M. Beck, D. E. Powers, J. B. Hopkins, and R. E. Smalley, J. Chem. Phys. 73 (1980) 2019.
16. S. M. Beck, J. B. Hopkins, D. E. Powers, and R. E. Smalley, J. Chem. Phys. 74 (1981) 43.
17. F. M. Behlen, D. B. McOonald, V. Sethuraman, and S. A. Rice, J. Chem. Phys. 75 (1981) 5685.
18. J. A. Warren, J. M. Hayes and G. J. Small, Anal. Chem. 54 (1982) 138.
19. J. M. Hayes and G. J. Small, Anal. Chem. 54 (1982) 1202.

20. M. Fuji, T. Ebata, N. Mikami and M. Ito, Chem. Phys. 77 (1983) 191.

21. J. S. Berlin, In Landolt-Börnstein Tables (Springer-Verlag, Berlin, 1951).

SECTION II. VIBRONIC MODE MIXING IN THE S_1 STATE OF β-METHYLNAPHTHALENE

ABSTRACT

Single vibronic level (SVL) fluorescence spectra of β-methylnaphthalene in supersonic expansions of helium are analyzed in terms of an excited state normal coordinate (Duschinsky) rotation and vibronically induced anharmonicity. Model calculations reveal that the application of simple first order corrections to the vibronic wavefunctions under a Duschinsky rotation reproduces most of the structure observed in the SVL spectrum of the naphthalenic Herzberg-Teller level $\bar{8}^1$ which is extensively mixed in β-methylnaphthalene. Discrepancies in the model are shown to be likely the result of anharmonicities. Manifestations of the Duschinsky rotation in rotationally resolved excitation spectra and in synchronously scanned excitation spectra are also discussed.

INTRODUCTION

Recently (1), we reported on the appearance of vibronically induced mode mixing in the S_1 state of β-methylnaphthalene and the resulting absorption/fluorescence mirror symmetry breakdown (MSB). The observed mode mixing, as manifested in single vibronic level (SVL) fluorescence spectra, was too extensive for a determination of the source of the mixing from our experimental data. We postulated, however, that the likely inducing mechanism was either a Duschinsky rotation (2) of excited state normal coordinates or vibronically induced anharmonicity, or possibly both. Since the determination of the source of the mode mixing is vital for the analysis of the spectral behavior of the molecule and since the prediction of its occurrence in related species is also important, we have reinvestigated the laser jet spectra of β-methylnaphthalene with the intent to quantify, or at least model, the mode mixing on the basis of the two mechanisms above.

Absorption/fluorescence MSB arising from excited state mode mixing appears to be generally more prevalent than was once thought. Several recent laser jet studies have revealed significant absorption/fluorescence asymmetries in a variety of species (3,4). However, only the S_2 state of azulene (4) has been demonstrated to show the degree of mode mixing comparable to that in β-methylnaphthalene. Furthermore, though mode mixing is the most commonly given explanation for MSB, there is seldom sufficient data provided to allow for a complete quantitation of the effect.

The laser jet spectra of β-methylnaphthalene are particularly intriguing in view of the fact that the parent molecule, naphthalene, displays no evidence of mode mixing in the gas phase (5). Yet, the SVL spectra of low energy S_1 vibronic levels in the β-methylated species show extensive mixing in the form of complicated multiplet fluorescence bands (1). In our earlier study (1), this mixing was taken to be responsible for the observed weakness of the excitation transition corresponding to $\bar{8}_0^1$ in naphthalene and the result of symmetry reduction of the molecule upon β-methylation. In this study, we focus on the source of the mode mixing and use data obtained from excitation spectra (both "low" resolution and rotationally resolved) and dispersed fluorescence (both origin and vibronically excited) of β-methylnaphthalene and β-methylnaphthalene-d_{10} to attempt to model the mixed mode behavior in the SVL fluorescence spectrum of $\bar{8}^1$.

EXPERIMENTAL

The rotationally cooled laser induced fluorescence (RC-LIF) apparatus used here is similar to that used in our earlier study (1), but several modifications have been made to improve sensitivity and reduce noise. These modifications are described elsewhere (6). β-Methylnaphthalene (Fluka, 97%) and β-methylnaphthalene-d_{10} (MSD Isotopes, 99.1%) are used without further purification.

RESULTS AND DISCUSSION

In this manuscript, assignments of transitions and vibrational sublevels of vibronic states are based on a standard notation scheme. Transitions between S_0 and S_1 involving changes in vibrational quanta in a given mode are denoted X_{ℓ}^{m} where the transition involves ℓ quanta of mode X in the ground state and m quanta in S_1. The appearance of a mode designation with only a superscript or only a subscript implies that we are referring to a vibronic state in S_1 or S_0, respectively, and not a transition.

In many instances, we are able to identify β-methylnaphthalene transitions as analogues to bands observed in naphthalene. Where possible, vibrational modes which are, thus, primarily "naphthalenic" are identified using the mode notation scheme which is standard for the latter molecule. There, vibrational mode numbers are pure and "barred" for modes of a_g and b_{1g} symmetry, respectively. In the S_1 state of β-methylnaphthalene, mode mixing precludes assigning vibrational sublevels to pure normal modes associated with the ground state. Thus, for example, transitions labeled as $\bar{8}_0^1$ should be recognized as transitions involving the excited state level $\bar{8}^1$ which is heavily mixed with other modes.

An example of excited state mode mixing manifested in SVL fluorescence is shown in Fig. 1. The pumped vibronic band (X_0^1) lies 477 cm^{-1} blue of the $S_0 \rightarrow S_1$ 0_0^0 band (31705 cm^{-1}) of β-methylnaphthalene. In addition to the resonant fluorescence transition (X_0^1), the spectrum

Figure 1. SVL fluorescence spectrum of the 477 cm^{-1} S_1 band of β-methylnaphthalene. Band positions are displayed relative to the S_0 origin. Resolution is 6 cm^{-1}. Sample temperature is 42°C. Helium backing pressure is 2 atm.

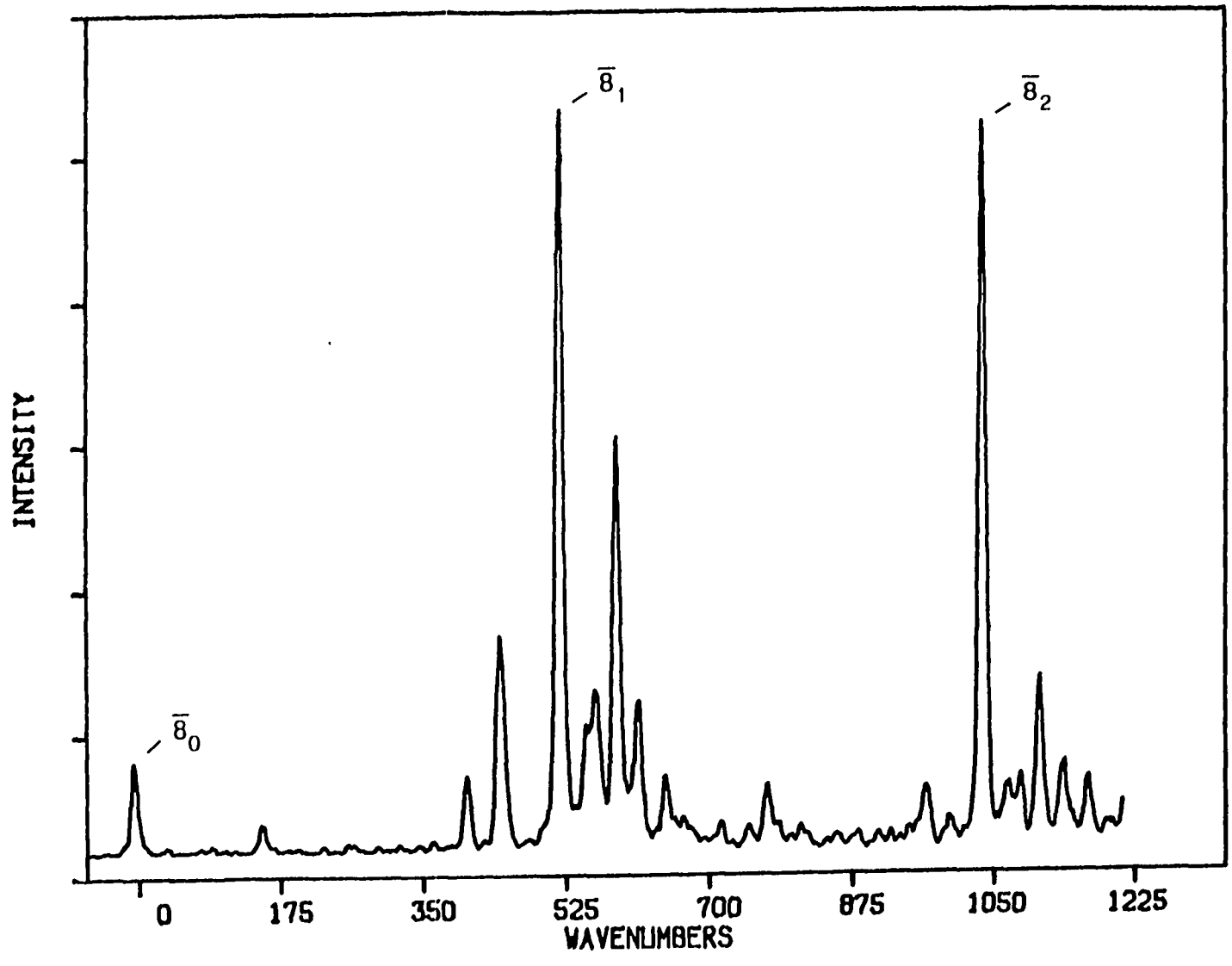
INTENSITY
$\bar{8}_0$
$\bar{8}_1$
$\bar{8}_2$
0
175
350
525
700
875
1050
1225
WAVENUMBERS

shows an extended multiplet in the region where one expects to see Δv_x = 0 or "one-to-one" (X_1^1) fluorescence. Further to the red, 0^0-type fluorescence is built off of the X_1^1 multiplet with each member of the multiplet acting as a false origin. The region containing the intense $X_1^1\bar{8}_1^0$ transitions is shown in Fig. 1. In the absence of mode mixing, only the three bands X_0^1, X_1^1, and $X_1^1\bar{8}_1^0$ should appear in the figure. Instead, as many as thirteen features make up the extended X_1^1 multiplet alone, implying that the excited state level possesses fractional excitation in as many ground state vibrational levels. [We note that in our original study (1), only three features were resolved in this region.] X^1 is, thus, best represented by $\{X\}^1$ where $\{X\}$ is a weighted set of thirteen ground state vibrational modes. The principal component to $\{X\}$ is the 519 cm^{-1}fundamental corresponding to the strong Herzberg-Teller inducing mode $\bar{8}$ in naphthalene (5) and we, therefore, assign the pumped level in S_1 to $\bar{8}^1$. The coupling of this mode to other vibrational levels in the S_1 state of β-methylnaphthalene results in its greatly reduced intensity in excitation, as seen in Fig. 2.

The SVL spectra (Figs. 3-7) of the five other nearby bands in the excitation spectrum (at 384, 417, 427, 448, and 484 cm^{-1}) display similar multiplets. In each, one band dominates in the X_1^1 multiplet allowing for a rough correspondence (Table 1) between the pumped levels in S_1 and their counterpart vibrational states in S_0. From their SVL spectra, it can be seen that mixing with $\bar{8}$ is present in each of the six S_1 bands with the exception of that at 417 cm^{-1}. Other S_1 vibronic levels of

Figure 2. Portion of the photoexcitation spectrum of β-methylnaphthalene. Band positions are displayed relative to the 0_0^0 band at 31705 cm^{-1}. The intensity of the 8_0^1 band is approximately 0.17 of the origin feature. The band marked α is due to an impurity of α-methylnaphthalene. T = 25°C. P_{He} = 2 atm.

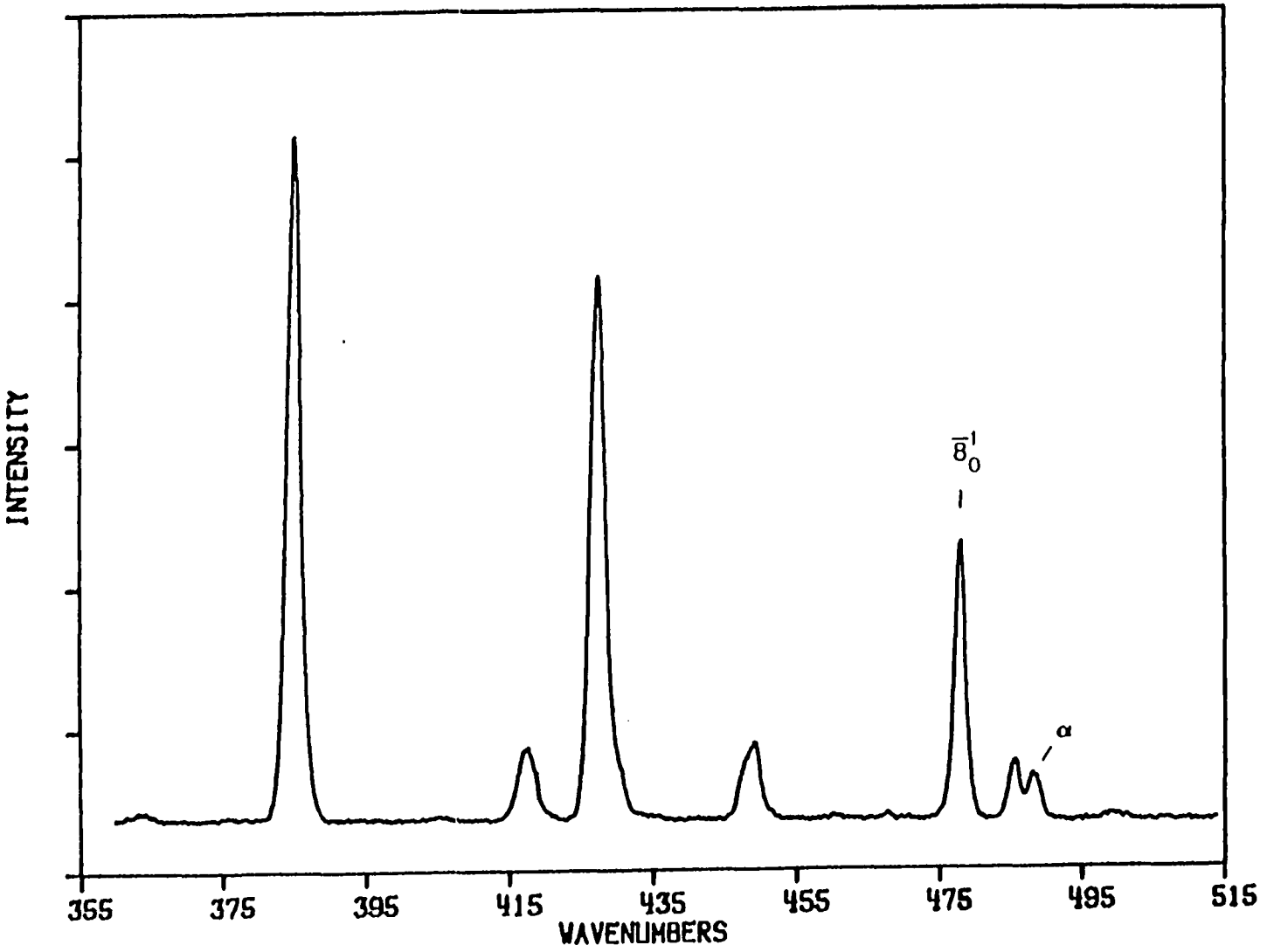
INTENSITY
$\overline{18}_0^1$
α
355
375
395
415
435
455
475
495
515
WAVENUMBERS

Figure 3. SVL fluorescence spectrum of the 384 cm^{-1} S_1 band of β-methylnaphthalene. Band positions are displayed relative to the S_0 origin. Resolution is 6 cm^{-1}. Sample temperature is 42°C. Helium backing pressure is 2 atm.

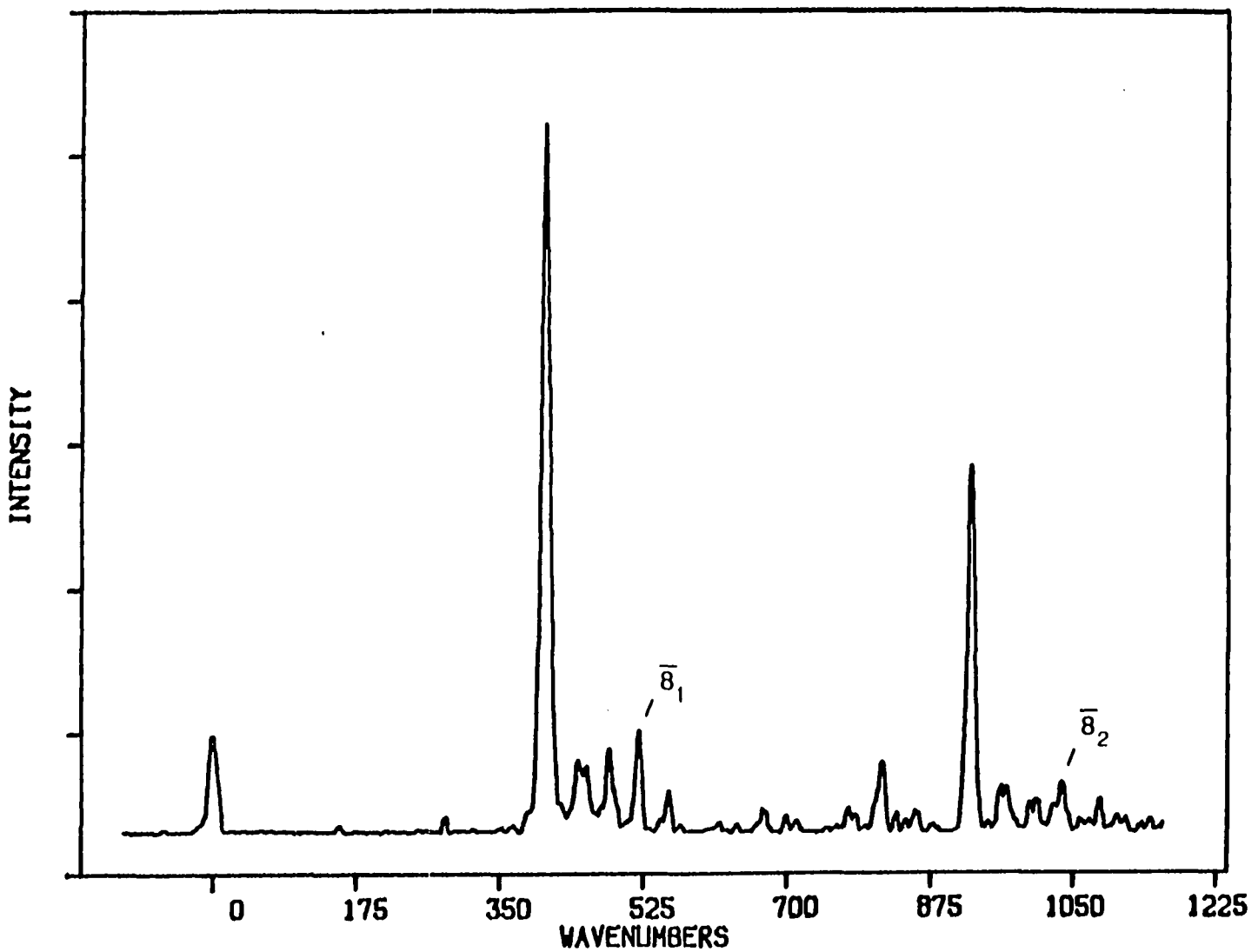
INTENSITY
$\bar{8}_1$
$\bar{8}_2$
0
175
350
525
700
875
1050
1225
WAVENUMBERS

Figure 4. SVL fluorescence spectrum of the 417 cm^{-1} S_1 band of β-methylnaphthalene. Band positions are displayed relative to the S_0 origin. Resolution is 6 cm^{-1}. Sample temperature is 42°C. Helium backing pressure is 2 atm.

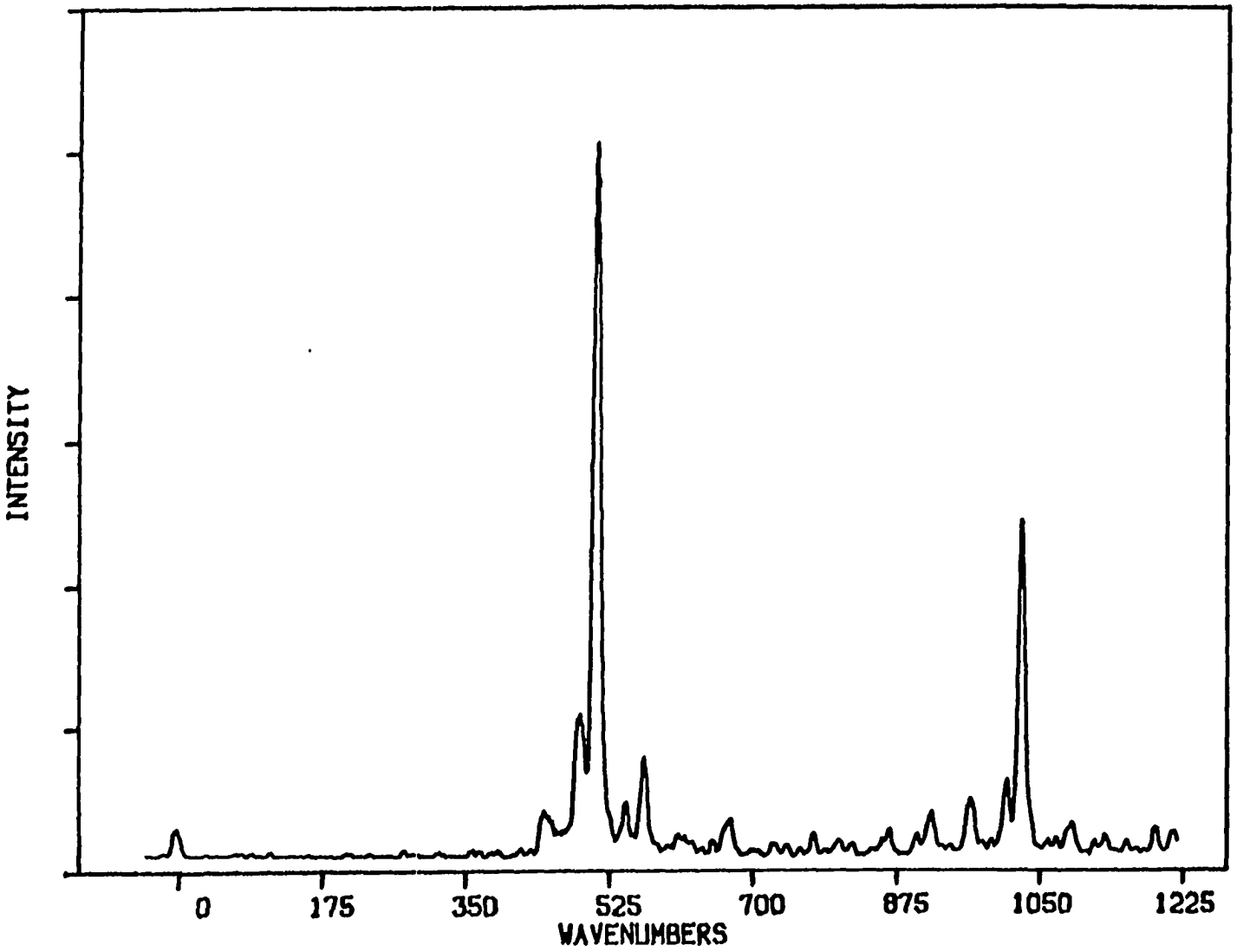
INTENSITY
0
175
350
525
700
875
1050
1225
WAVENUMBERS

Figure 5. SVL fluorescence spectrum of the 427 cm^{-1} S_1 band of β-methylnaphthalene. Band positions are displayed relative to the S_0 origin. Resolution is 6 cm^{-1}. Sample temperature is 42°C. Helium backing pressure is 2 atm.

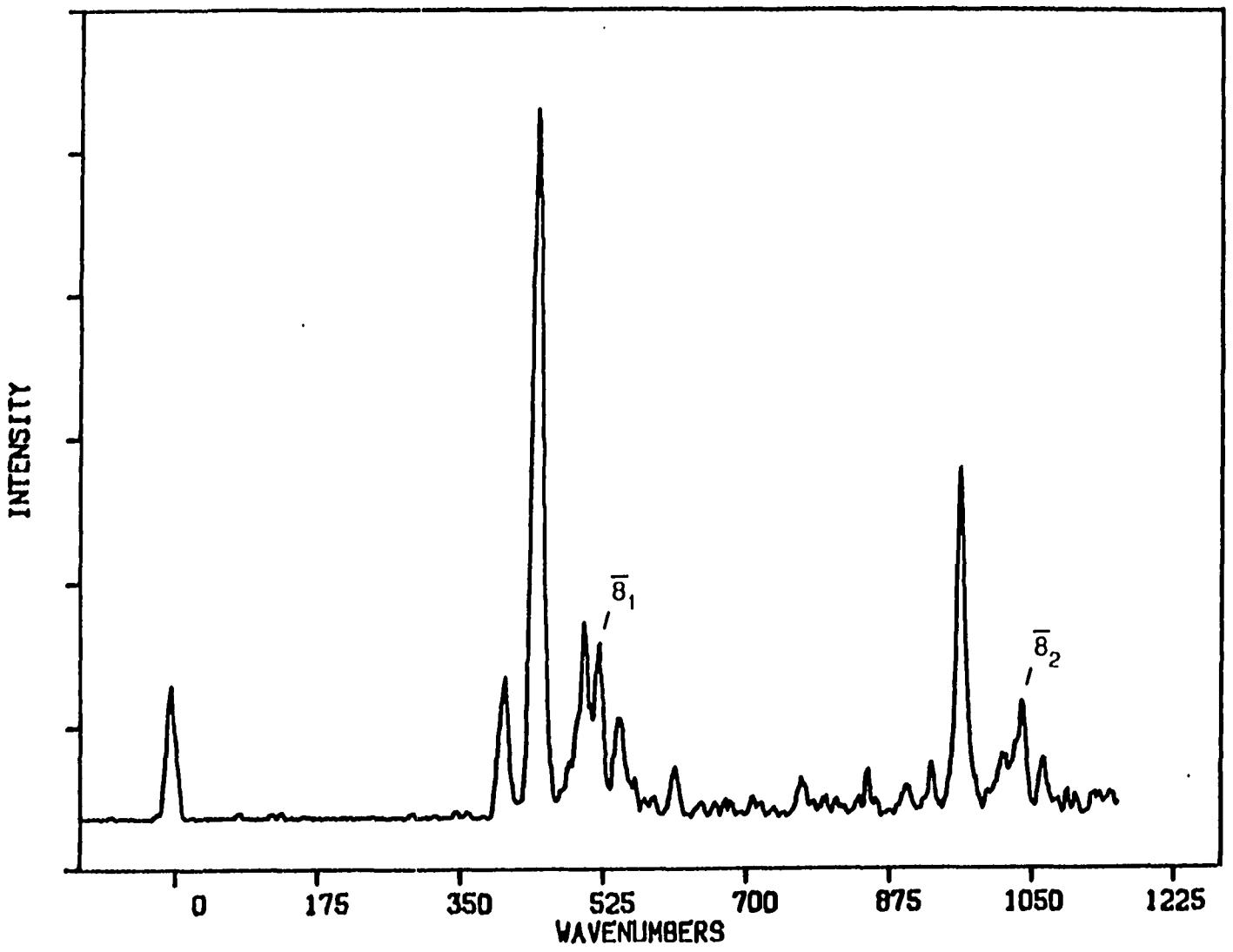
INTENSITY
$\bar{8}_1$
$\bar{8}_2$
0
175
350
525
700
875
1050
1225
WAVENUMBERS

Figure 6. SVL fluorescence spectrum of the 448 cm^{-1} S_1 band of β-methylnaphthalene. Band positions are displayed relative to the S_0 origin. Resolution is 6 cm^{-1}. Sample temperature is 42°C. Helium backing pressure is 2 atm.

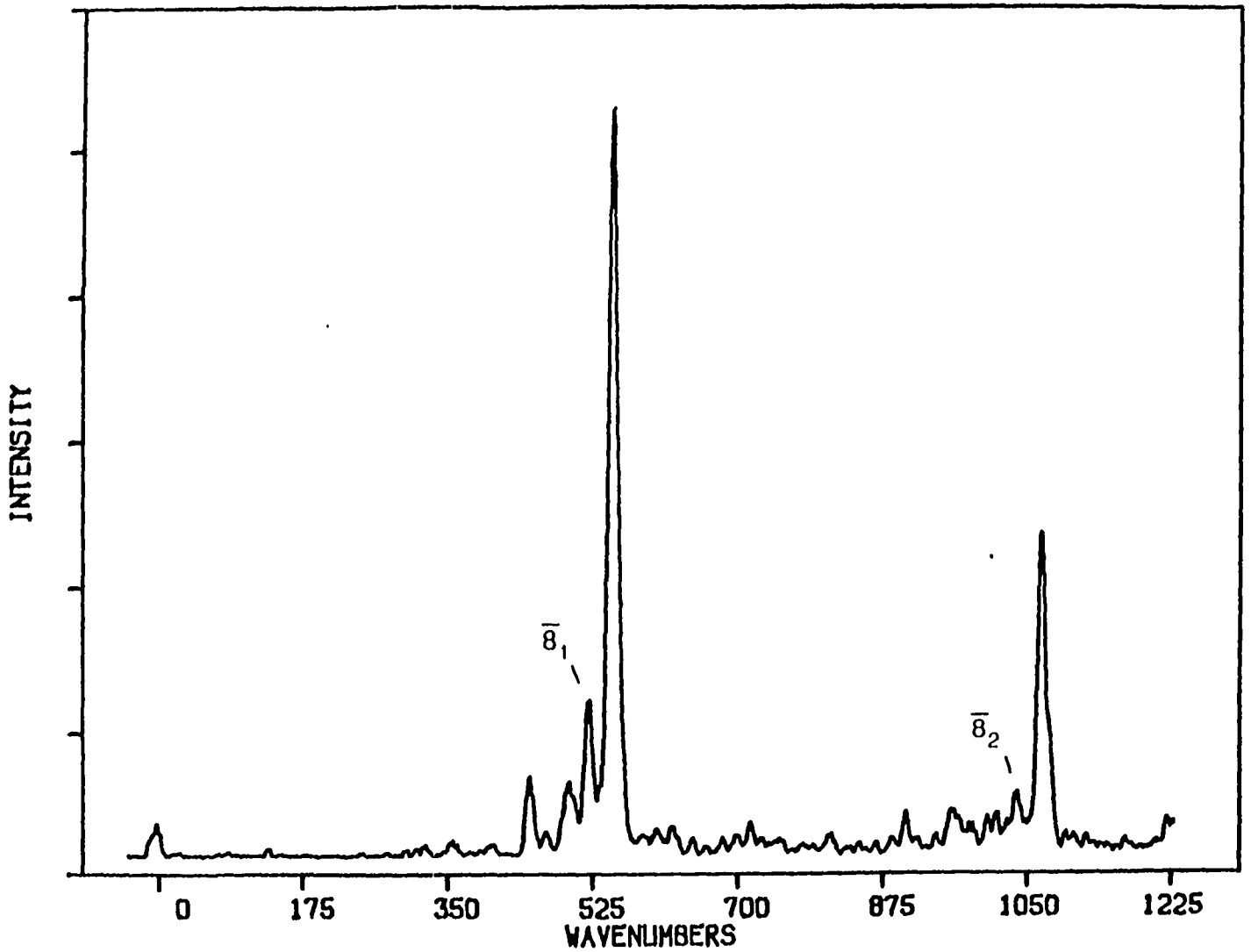
INTENSITY
$\bar{8}_1$
$\bar{8}_2$
0
175
350
525
700
875
1050
1225
WAVENUMBERS

Figure 7. SVL fluorescence spectrum of the 484 cm^{-1} S_1 band of β-methylnaphthalene. Band positions are displayed relative to the S_0 origin. Resolution is 6 cm^{-1}. Sample temperature is 42°C. Helium backing pressure is 2 atm.

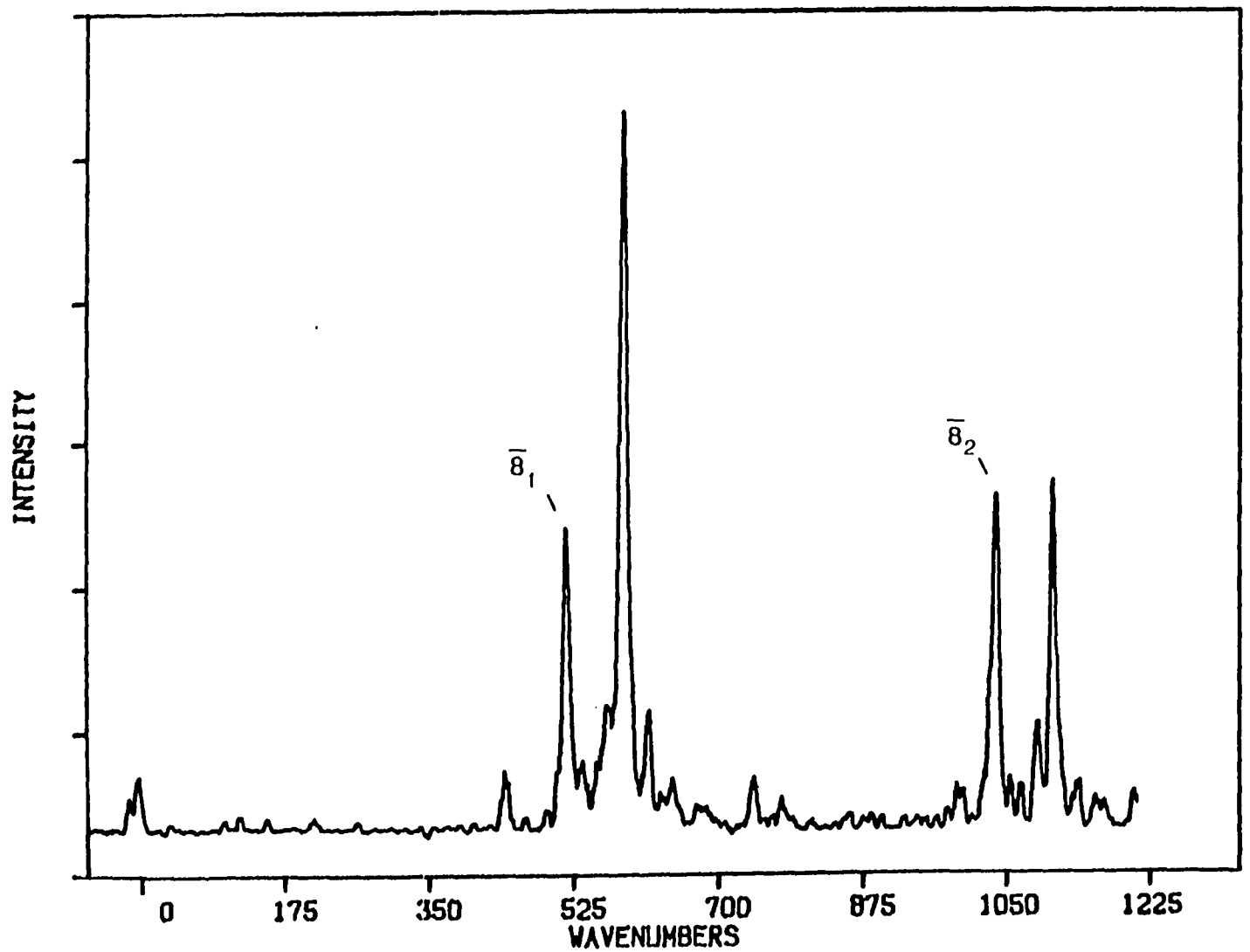
INTENSITY
$\bar{8}_1$
$\bar{8}_2$
0
175
350
525
700
875
1050
1225
WAVENUMBERS

Table 1. Excited and ground state vibrational frequencies obtained from the excitation and SVL fluorescence spectra in Figs. 1-7. Normalized 0^0-fluorescence intensities and band types are listed. Absolute values of the excited state mixing coefficients $D_{\beta\bar{8}}$ are also shown

ω_x' (cm^{-1})	ω_x (cm^{-1})	$I(x_1^0)/I(0_0^0)$	$\lvert D_{\beta\bar{8}}\rvert$
384	408	0.03 - Condon	0.39
417	513	<0.005 - Condon	0.00
427	449	0.01 - Condon	0.45
448	548	<0.005 - HT	0.44
477	519	0.38 - HT	----
484	590	<0.005 - HT	0.59

β-methylnaphthalene, particularly those to higher energy, show mixed mode behavior in SVL fluorescence (1), but we will here focus on only the six bands in the low energy (300-600 cm^{-1}) region. These bands are well isolated from others in the excitation spectrum and anticipating the application of perturbation theory, where vibronic state energy differences appear in the denominators of the coupling terms, it is hoped that analysis of these six bands alone will allow for a nearly complete modeling of their mixing.

At this point, we briefly review the spectral effects of a Duschinsky rotation of normal coordinates in the confines of the adiabatic harmonic oscillator approximation and relate it to the observed SVL spectrum in Fig. 1.

The term Duschinsky rotation (2) refers to the description of excited state normal coordinates, Q', as linear combinations of ground state normal coordinates, Q:

$$Q'_x = \sum_\alpha S_{x\alpha} Q_\alpha + \delta_x \qquad (1)$$

where the summation is carried over all coordinates of the same symmetry as Q_x. The origin displacements, δ, are nonzero only for totally symmetric vibrations unless a change in point group symmetry occurs upon excitation. In the case of β-methylnaphthalene, where the covering symmetry is C_s in both S_0 and S_1, we will nevertheless neglect all δ. The 0_0^0-excited fluorescence spectrum reveals strong Condon intensity

(indicating nonnegligible δ_x) in only one mode: the 1388 cm^{-1} S_0 vibration corresponding to 5_1 in naphthalene which we will not be concerned with here. This assumption also avoids accounting for absorption/fluorescence asymmetries resulting from Condon/Herzberg-Teller interferences (6). Furthermore, though the 0^0-fluorescence and Raman spectra of β-methylnaphthalene closely resemble those of naphthalene, indicating that the vibrational wavefunctions maintain a "sense" of D_{2h} symmetry in S_0, the excited state vibrations need not be as well behaved. As a result, we will consider here mixing among all of the 39 planar modes of β-methylnaphthalene.

To apply the Duschinsky rotation described by Eq. (1), we begin with the assumption that the zero order excited state vibrational wavefunctions, $|i\rangle$, are identical to their ground state counterpart wavefunctions. Thus, for example, $|\overline{8}^1\rangle = |\overline{8}_1\rangle$. The excited state levels are then corrected to first order (e.g., to $|\overline{8}^1\rangle'$) by

$$|i\rangle' = |i\rangle + \sum_{j\neq i} \frac{|j\rangle\langle j|V|i\rangle}{\varepsilon_i - \varepsilon_j} \qquad (2)$$

where ε_i and ε_j are zero order vibrational energies and the coupling potential

$$V = \frac{1}{2} \sum_{\substack{\alpha,\beta \\ \alpha\neq\beta}} B_{\alpha\beta} Q_\alpha Q_\beta \quad . \qquad (3)$$

The coefficients $B_{\alpha\beta}$ have been related (7,8) to the Herzberg-Teller (HT) vibronic coupling matrix elements in Q_α and Q_β and we, therefore, expect that strong HT inducing modes which are in near resonance will mix appreciably. This should be important in the case of substituted naphthalenes where a number of HT modes typically dominate the spectra.

Applying the above equations in the harmonic oscillator approximation to an excited state fundamental vibronic level X^1, we obtain

$$|X^1\rangle' = |X^1\rangle - \sum_{\beta \neq X} D_{\beta X}|\beta^1\rangle \tag{4}$$

where

$$D_{\beta X} = \left(\frac{\hbar}{2\omega_\beta}\right)^{1/2} \left(\frac{\hbar}{2\omega_X}\right)^{1/2} \frac{B_{\beta X}}{\hbar(\omega_\beta - \omega_X)} \tag{5}$$

and where we have neglected terms where the denominators include sums of vibrational frequencies. In obtaining Eqs. (4) and (5), we have made use of the common harmonic oscillator relation

$$Q_\beta|\beta^v\rangle = \left(\frac{v\hbar}{2\omega_\beta}\right)^{1/2} |\beta^{v-1}\rangle + \left(\frac{(v+1)\hbar}{2\omega_\beta}\right)^{1/2} |\beta^{v+1}\rangle \quad . \tag{6}$$

In contrast to the vibrational sublevels of the S_1 state, the zero-point level is largely unaffected by the Duschinsky rotation as no terms

are produced containing denominators with vibrational frequency differences. Therefore, its wavefunction can be taken to be the same as that for the zero-point level of the ground state. The 0^0-fluorescence spectrum will, thus, show little evidence of normal coordinate rotation, while Eqs. (4) and (5) will describe the mode mixing observed for excited state fundamentals. Relations analogous to Eq. (4) are readily generated for overtone and combination levels in S_1 by application of Eqs. (2) and (3) to the appropriate zero order wavefunctions. It is important to note here that the excited state vibrational wavefunctions generated remain harmonic with the use of harmonic zero order functions.

If we assume that the transition intensities in β-methylnaphthalene involve only Condon and HT contributions to the transition moments, then the intensities of bands observed in SVL fluorescence from $|X^1\rangle'$ described by Eq. (4) are given by

$$|\langle f|\underline{M}|X^1\rangle'|^2 = |\underline{M}_0\langle f|X^1\rangle - \sum_{\beta\neq X} D_{\beta X}\underline{M}_0\langle f|\beta^1\rangle + \sum_{\ell\neq X} \underline{m}_\ell\left(\frac{\hbar}{2\omega_\ell}\right)^{1/2}\langle f|X^1\ell^1\rangle$$

$$+ \underline{m}_X\left(\frac{\hbar}{2\omega_X}\right)^{1/2}\langle f|X^0\rangle + \sqrt{2}\,\underline{m}_X\left(\frac{\hbar}{2\omega_X}\right)^{1/2}\langle f|X^2\rangle$$

$$- \sum_{\ell\neq\beta}\sum_{\beta\neq X}\underline{m}_\ell\left(\frac{\hbar}{2\omega_\ell}\right)^{1/2}D_{\beta X}\langle f|\beta^1\ell^1\rangle - \sum_{\beta\neq X}\underline{m}_\beta\left(\frac{\hbar}{2\omega_\beta}\right)^{1/2}D_{\beta X}\langle f|\beta^0\rangle$$

$$- \sum_{\beta\neq X}\sqrt{2}\,\underline{m}_\beta\left(\frac{\hbar}{2\omega_\beta}\right)D_{\beta X}\langle f|\beta^2\rangle|^2 \qquad (7)$$

where $|f\rangle$ is the vibrational wavefunction of the terminating level in fluorescence. Here, we have made use of the usual expression (9) for the first order transition moment:

$$\underline{M} = \underline{M}_0 + \underline{m}_x Q_x \tag{8}$$

where $\underline{M}_0$ and $\underline{m}_x$ are the Condon and Herzberg-Teller induced electronic transition moments, respectively.

To model the SVL spectra of β-methylnaphthalene under the influence of a Duschinsky rotation, a determination of the coupling parameters, $D_{\beta x}$, and the zero order spectral behavior are needed. The latter can be obtained by analysis of the 0_0^0-excited fluorescence spectrum (Fig. 8) by analogy with naphthalene. In both species, intense fundamental transitions are observed in $\overline{8}_1^0$, $\overline{7}_1^0$, 8_1^0, and 7_1^0 at 519, 956, 771 and 1025 cm^{-1}, respectively, in β-methylnaphthalene and at 506, 939, 769 and 1017 cm^{-1}, respectively, in naphthalene. They obtain intensity primarily via HT coupling of S_1 with S_2 (for $\overline{8}$ and $\overline{7}$) and S_4(for 8 and 7). The fact that their relative intensities do not change despite the strong enhancement of the 0_0^0 band upon methylation indicates that the Condon contributions to these bands in β-methylnaphthalene remains negligible. Only the 0_0^0 and 5_1^0 bands possess significant Condon intensity. Similarly, while a few new weak transitions appear in the β-methylnaphthalene spectrum, the vibrational frequencies of the ground state naphthalenic modes identifiable in the spectrum are shifted only slightly (0 to 15

Figure 8. SVL fluorescence spectrum of the 0_0^0 band of β-methylnaphthalene. Band positions are displayed relative to the S_0 origin. Resolution is 6 cm^{-1}. Sample temperature is 42°C. Helium backing pressure is 2 atm.

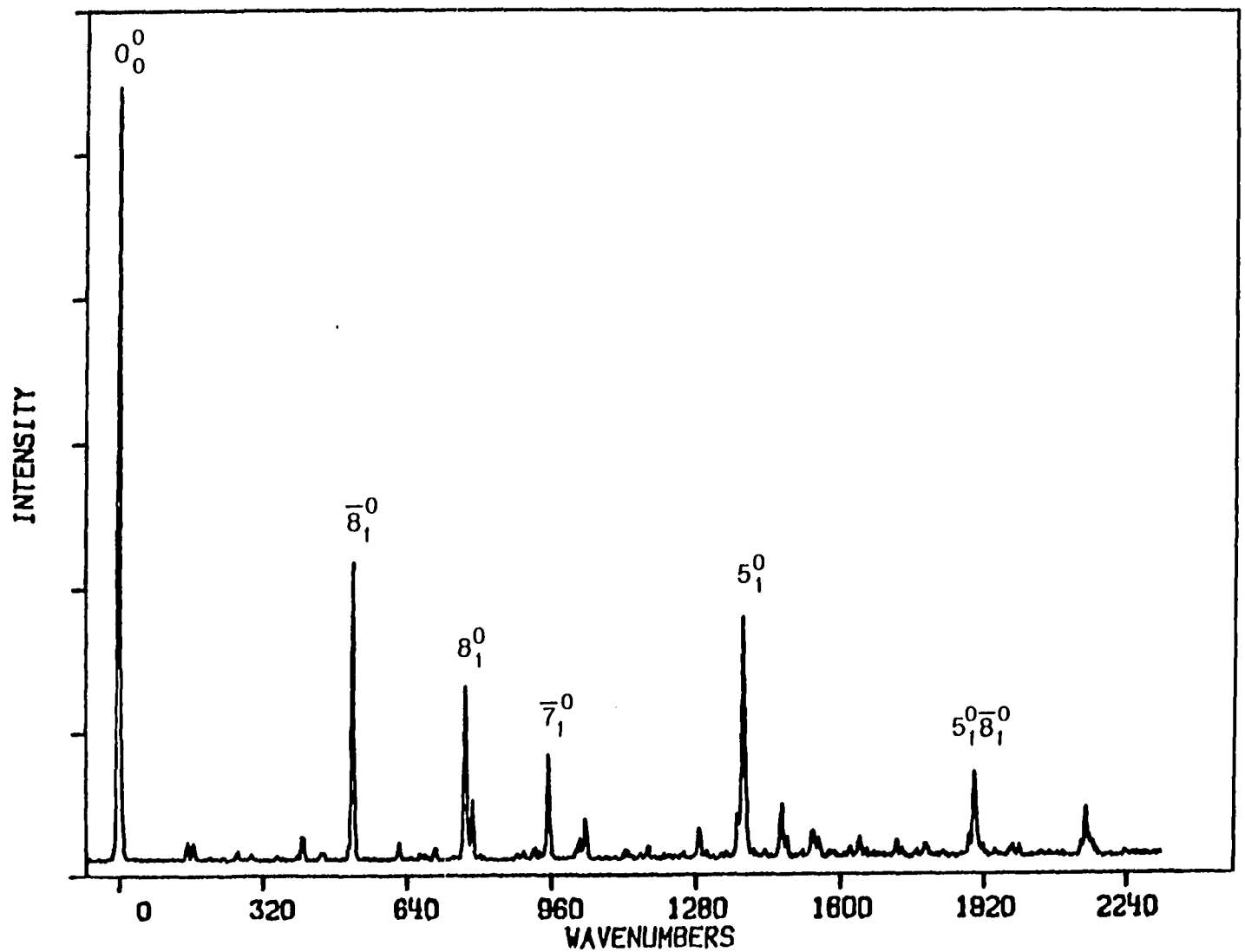
0_0^0
$\bar{8}_1^0$
8_1^0
$\bar{7}_1^0$
5_1^0
$5_1^0\bar{8}_1^0$
INTENSITY
0
320
640
960
1280
1600
1920
2240
WAVENUMBERS

cm^{-1}) relative to the parent molecule. As a result, we deem it appropriate to use the available data on naphthalene where needed since we know of no reliable vibrational analyses of β-methylnaphthalene, and since the above results indicate that the methyl group acts only as a minor perturbation to the nuclear Hamiltonian in S_0.

The intensities of the β-methylnaphthalene 0^0-fluorescence bands terminating in the six S_0 vibrational levels of concern are listed in Table 1. Aside from the intense HT band $\bar{8}_1^0$ at 519 cm^{-1}, each of these transitions is weak. In order to simplify the spectral modeling, we assume that each is either entirely Condon or entirely HT induced. In the case of Condon transitions, the intensity is proportional to the square of the Franck-Condon integral $\langle X_1|X^0\rangle$. From it, all Franck-Condon integrals of the type $\langle X_v|X^{v'}\rangle$ can be calculated in the harmonic oscillator approximation (10). For the HT bands, the intensity is related to

$$\left(\frac{\vec{m}_x}{\vec{M}_0}\right)^2 \langle X_1|X^1\rangle^2 \equiv \left(\frac{\vec{m}_x}{\vec{M}_0}\right)^2 \quad . \tag{9}$$

To determine which is the contributing factor for a given 0^0-fluorescence band, we turn to the high resolution (0.05 cm^{-1}) scans (Fig. 9) of the corresponding bands in photoexcitation. Rotational contours of transitions which appear to be predominantly long axis polarized (possessing a central Q-branch pileup in the band envelope as in 0_0^0) are assumed to be Condon bands. Transitions which are short axis polarized

Figure 9. Rotational contours of bands in photoexcitation. Contours 'a' through 'g' are of the 0, 384, 417, 427, 448, 477, and 484 cm^{-1} features, respectively. The intensity scale differs for each band. Excitation energy increases to the left in each. Resolution is <0.08 cm^{-1}. T = 61°C. P_{He} = 2 atm.

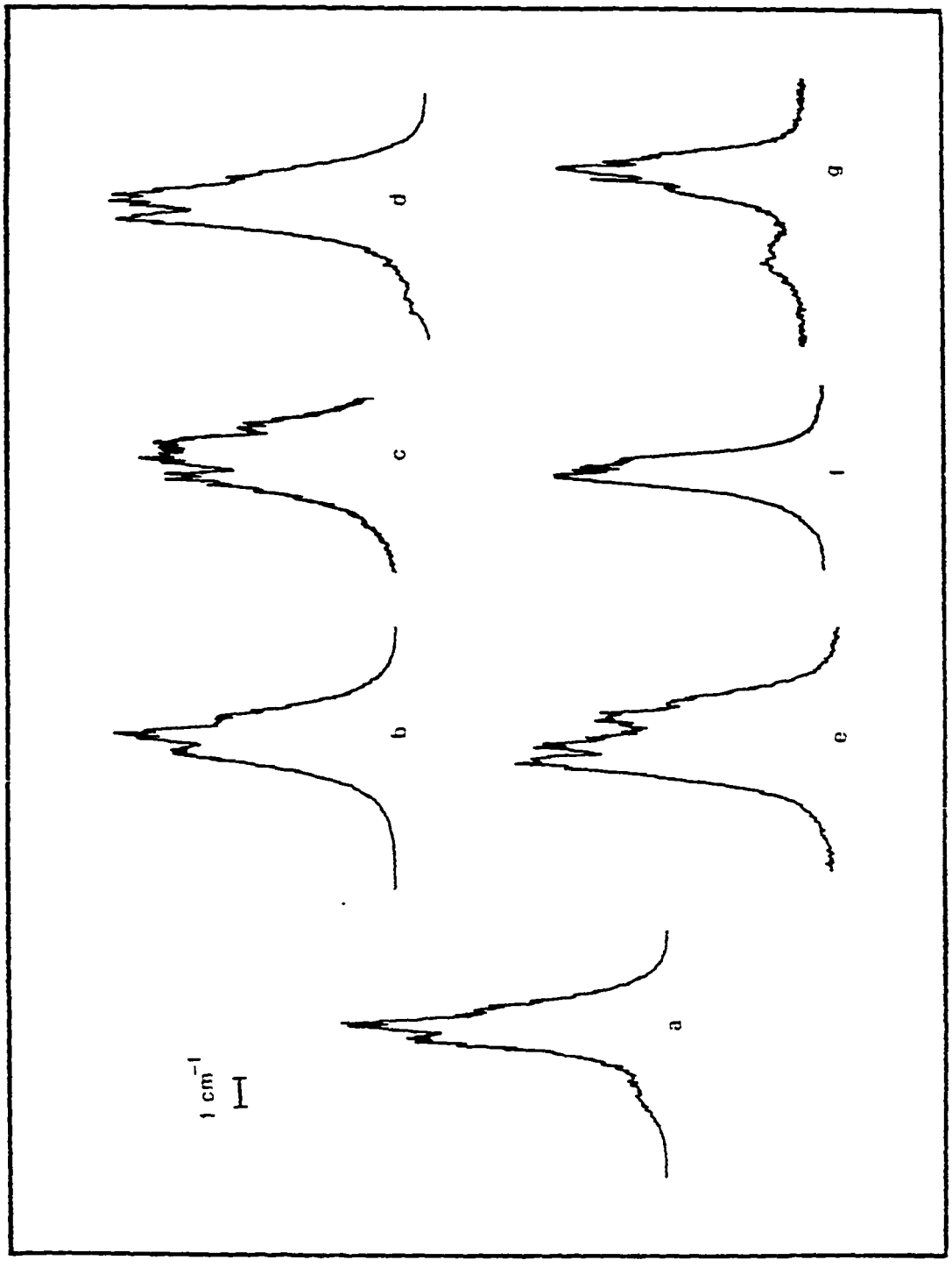
1 cm⁻¹
a
b
c
d
e
f
g

are taken as HT induced. While the latter assignments should be correct in most cases involving planar fundamentals, assignments of the former as Condon bands is questionable. In naphthalene, the intense transitions involving the totally symmetric modes 7 and 8, for example, obtain most of their intensity via vibronic coupling but would reveal long axis polarization because of their symmetry. However, as can be seen from Fig. 9, each rotational contour observed is different with no band revealing purely long axis or purely short axis polarization. In the absence of adequate rotational constant data, we forego any detailed analyses of these spectra. We do note, however, that if the observed Duschinsky rotation mixes all planar modes of the molecule, then a mixing of transition polarization is a necessary result. In a species with known rotational constant information, an analysis of the contours in photoexcitation could, thus, reveal the degree of mixing in modes of different polarization.

In order to model the SVL spectrum of a given vibronic level $|X^1\rangle$, we now require a determination of the coupling parameters $D_{\beta x}$. Lacking independent sources, we obtain these from analysis of the SVL fluorescence spectra of the vibronic levels to which the level is coupled.

We here choose to attempt to model the SVL spectrum (Fig. 1) of the 477 cm^{-1} S_1 level of β-methylnaphthalene. The principal counterpart of this level in S_0 is the strong HT inducing mode $\overline{8}_1$ at 519 cm^{-1}. From the spectra shown in Figs. 3-7, we obtain values of $|D_{\beta\overline{8}}|$ for each of the remaining five vibronic levels in the S_1 300-600 cm^{-1} region.

In Table 2, we compare the relative intensities of the SVL fluorescence of Fig. 1 calculated using Eq. (7) and the data presented with the observed intensities. A reasonable correlation is seen for most of the bands in the spectrum. Clearly, the first order corrections to the excited state vibronic level $\overline{8}^1$ reproduce most of the structure observed in its SVL fluorescence spectrum and, thus, adequately describes most of its mixing with other levels in S_1. We also note that the use of the tabulated values of $|D_{\beta\overline{8}}|$ and of ground state vibrational frequencies in Eq. (5) gives values of $|B_{\beta\overline{8}}|^{1/2}$ of roughly 100 to 200 cm^{-1} for the levels β considered. Such values are consistent for the intense HT naphthalenic $\overline{8}$ mode mixed with a fundamental of weak or moderate HT activity (7,8).

The disparities between the observed and calculated spectra in Table 2 occur principally in the form of bands present in the observed spectrum which are not predicted by the model. Clearly, the inclusion of more coupled zero order vibrational states could resolve the discrepancies but this produces a more serious problem. Not all of the transitions in the "one-to-one" multiplet region can terminate in ground state fundamentals. The density of planar modes in 3-methylnaphthalene is insufficient. Instead, some of the bands must involve overtone or combination levels. Transitions to these levels in SVL fluorescence are, however, predicted to be very weak under a simple Duschinsky rotation and we must account for their intensities by other means.

Table 2. Observed and calculated intensities for the SVL fluorescence spectrum of $\bar{8}^1$. Band intensities are normalized to the $\bar{8}_1^1$ transition

ω (cm^{-1})	Intensities	
	Observed	Calculated
0	12	
154	5	
407	11	15
448	29	20
513	0	0
520 ($\bar{8}_1$)	100	100
550	17	19
563	22	
590	54	38
617	23	
648	11	
717	4	
750	4	
772	8	
814	4	
926 ($\bar{8}_1$ + 407)	0	6
969 ($\bar{8}_1$ + 448)	8	8
998	6	
1032 ($\bar{8}_1$ + 513)	0	0
1039 ($\bar{8}_2$)	99	77
1070 ($\bar{8}_1$ + 550)	9	7
1084	11	
1109 ($\bar{8}_1$ + 590)	15	15
1138	13	
1169	11	

The presence of bands terminating at 154, 407, 562, 717, and 969 cm^{-1} in S_0 is of particular interest. These can be readily assigned as A_1, B_1, A_1B_1, A_2B_1, and A_1B_2 vibrational levels where A and B are unidentified fundamentals. In order for all five bands to appear in the SVL spectrum with nonzero intensity, the pumped state must mix with the zero order $|A^1B^1>$ state. This requires a significant anharmonicity in S_1 vibronic levels.

The occurrence of strong third order vibronically induced anharmonicity results in a similarly extensive mode mixing in the S_2 state of azulene (4,11). However, in β-methylnaphthalene, we must include higher order coupling to account for the observed mixing. This becomes apparent when the vibrational levels A and B are identified. In the preceding paragraph we assigned the 154 cm^{-1} S_0 vibration to A_1. The excitation spectrum of β-methylnaphthalene reveals bands at 100 and 123 cm^{-1} (76 and 82 cm^{-1} in β-methylnaphthalene-d_{10}) with counterparts in 0^0-fluorescence at 152 and 164 cm^{-1} (unresolved at 119 cm^{-1} in the deuterated species). The large isotope shifts for these transitions indicate that they are overtones of the methyl torsion mode and, thus, the vibration A_1 is actually T_2. The pumped vibronic level must, therefore, mix with $|T^2B^1>$ which requires inclusion of anharmonicities to fourth order in Q (9,11).

At this point, it should be clear that further modeling of the spectra of β-methylnaphthalene would require considerably more detailed vibronic data than we have available. For example, transition intensities observed in excitation will depend sensitively on the relative

signs of the coupling parameters $D_{\beta x}$ and of $\underline{m}_{\beta}/\underline{M}_{0}$ in addition to their magnitudes. An added complication arises when $\underline{m}_{\beta}$ and $\underline{m}_{x}$ are perpendicular (or simply nonparallel) which will occur in β-methylnaphthalene if modes which are of b_{1g} and a_{g} symmetry in naphthalene are mixed. While it will be seen that the excitation intensity of a given transition (e.g., $\overline{8}_{0}^{1}$) will be increased or decreased as a result of a Duschinsky rotation, the inclusion of several nonnegligible terms of varying magnitude and sign in the transition moment equation makes it difficult to make reasonable estimates of excitation intensities.

The contribution of an intensity "source" for excitation transitions can, however, be probed by synchronous excitation scans of the pump laser and detection monochromator. In Fig. 2, we show the excitation spectrum over the low energy region of β-methylnaphthalene using an unfiltered photomultiplier tube detector. In Fig. 10, a detection monochromator is stepped synchronously with the pump laser maintaining a frequency separation of 519 cm^{-1}. Thus, S_1 vibronic bands appear in the spectrum with intensities related to their absorption intensities and their yields of fluorescence to $\overline{8}_{1}$. Vibronic levels which carry finite contributions from $\overline{8}^{1}$ can, thus, be readily identified. Though the spectrum provides no additional information to that contained in the excitation and SVL spectra, it does provide a means of determining the extent of intensity "dilution" from mode mixing of a given excitation transition in a single spectrum.

Figure 10. Same as Fig. 2 with synchronous scanning of the detection monochromator 519 cm^{-1} "red" of the laser. Monochromator bandpass is 5 cm^{-1}

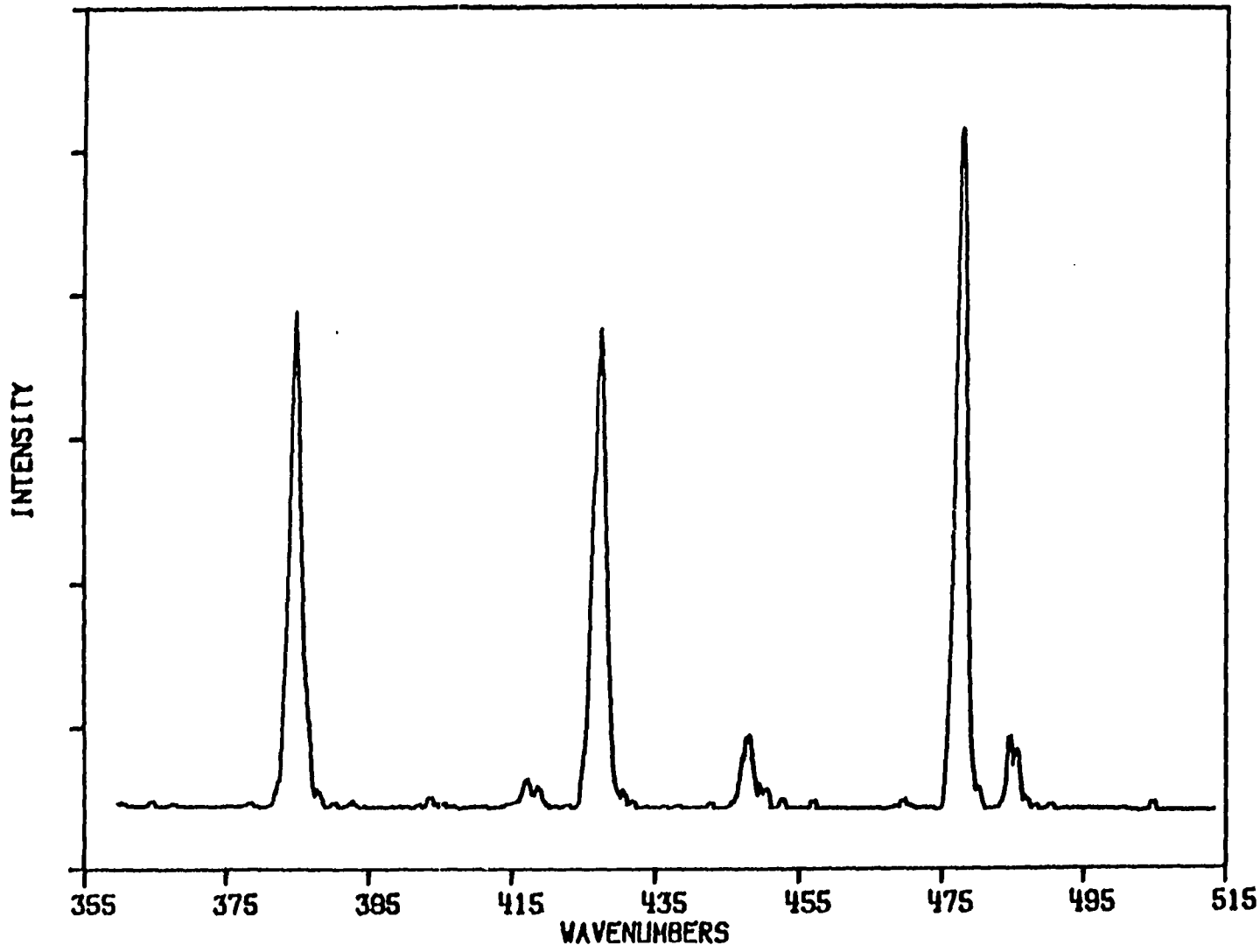
INTENSITY
355
375
395
415
435
455
475
495
515
WAVENUMBERS

CONCLUSIONS

On the basis of the model calculations presented, the observed S_1 mode mixing in β-methylnaphthalene can be accounted for primarily by a Duschinsky rotation of normal coordinates. Though the mixing is extensive, the application of first order corrections to the excited state vibrational sublevel $\overline{8}^1$ clearly accounts for the majority of the structure observed in SVL fluorescence. Discrepancies between the calculated and observed spectra are likely the result of excited state anharmonicities to third and fourth order. Further details of the mixing are available from rotationally resolved excitation spectra and synchronously scanned excitation spectra provided that sufficient information concerning the rotational states and zero order normal mode structure are learned.

REFERENCES

1. J. A. Warren, J. M. Hayes, and G. J. Small, J. Chem. Phys. 80 (1984) 1786.

2. F. Duschinsky, Acta Physicochim. 7 (1937) 551.

3. See, for example, (a) A. R. Auty, A. C. Jones, and D. Phillips, Chem. Phys. Lett. 112 (1984) 529; (b) I. Y. Chan and M. Dauts, J. Chem. Phys. 82 (1985) 4771; (c) T. Ebata, Y. Suzuki, N. Mikami, T. Miyashi, and M. Ito, Chem. Phys. Lett. 110 (1984) 597; (d) J. Subbi, Chem. Phys. Lett. 109 (1984) 1; (e) D. Klapstein, R. Kuhn, J. P. Maier, M. Ochsner, and W. Zamback, J. Phys. Chem. 88 (1984) 5176; (f) A. Oikawa, H. Abe, N. Mikami, and M. Ito, J. Phys. Chem. 88 (1984) 5180.

4. M. Fujii, T. Ebata, N. Mikami, and M. Ito, Chem. Phys. 77 (1983) 191.

5. (a) M. Stockburger, H. Gattermann, and W. Klusmann, J. Chem. Phys. 63 (1975) 4519; (b) S. M. Beck, D. E. Powers, J. B. Hopkins, and R. E. Smalley, J. Chem. Phys. 73 (1980) 2019; (c) S. M. Beck, J. LB. Hopkins, D. E. Powers, and R. E. Smalley, J. Chem. Phys. 74 (1981) 43.

6. J. A. Warren, J. M. Hayes, and G. J. Small, Chem. Phys., submitted.

7. G. J. Small, J. Chem. Phys. 54 (1971) 3300.

8. B. Sharf and B. Honig, Chem. Phys. Lett. 7 (1970) 132.

9. G. Fischer, In Vibronic Coupling (Academic Press, London, 1984).

10. J. R. Henderson, M. Muramoto, and R. A. Willett, J. Chem. Phys. 41 (1964) 580.

11. A. R. Lacey, E. F. McCoy, and I. G. Ross, Chem. Phys. Lett. 21 (1973) 233.

SECTION III. VIBRONIC ACTIVITY IN THE LASER JET SPECTRA OF PHENANTHRENE

ABSTRACT

Photoexcitation and dispersed fluorescence spectra of phenanthrene and phenanthrene-d_{10} in supersonic expansions of helium are presented. Mirror symmetry breakdown (MSB) between excitation and S_1 origin excited fluorescence is quantified for transitions involving planar vibrational modes. For modes which are totally symmetric, model calculations are performed based on the formalism of Craig and Small (J. Chem. Phys. 50 (1969) 3827) for the interference of Condon and Herzberg-Teller derived transition moments. It is shown that for a_1 transitions displaying drastic absorption/fluorescence asymmetries, observed intensities can be reproduced by use of simple first order formulae. The breakdown of the model in predicting the 20_0^1 (632 cm^{-1} in S_1) and 20_1^0 (679 cm^{-1} in S_0) transitions in phenanthrene-d_{10} is discussed. Mode mixing is observed in several b_2 levels and in a_1 levels near 1380 cm^{-1} in S_1 and are described in terms of normal coordinate (Duschinsky) rotation and Fermi resonance, respectively.

INTRODUCTION

Recently (1,2), we reported on the appearance of absorption/fluorescence mirror symmetry breakdown (MSB) resulting from excited state mode mixing in β-methylnaphthalene. Much of our interest in vibronically induced MSB has stemmed from the abundance of recent laser jet studies which report significant asymmetries in the spectra obtained for a number of polyatomic molecules (3). The ability to obtain spectra of isolated species in supersonically cooled expansions allows for the study of vibronic activity by analysis of its manifestation in photoexcitation and single vibronic level (SVL) fluorescence spectra. Indeed, such studies can now provide valuable tests for a number of models of vibronically induced MSB. This contrasts with condensed phase studies where absorption/fluorescence asymmetries are affected by guest/host interactions and unrelaxed fluorescence spectra are not generally available.

Most commonly, intrinsic MSB is ascribed to mode mixing, as a result of either a Duschinsky rotation (4-6) of excited state normal coordinates or a Fermi resonance, though there is often little substantiating evidence provided. Since MSB seems to be more prevalent in polyatomics than was once thought, it seems important that caution be used in accounting for spectral asymmetries by any single mechanism. In our studies of β-methylnaphthalene, for example, we attempted to model the observed spectra with inclusion of vibronically induced mode mixing via both of these mechanisms, but noted that the spectra showed evidence of other contributions to the asymmetries.

In species of low symmetry particularly, one possible source of MSB involves interference of the Condon "allowed" and vibronically induced moments for transitions involving totally symmetric vibrations. This interference has been noted to result in strong asymmetries in the band intensities of phenanthrene (7) while its contribution to the spectra of other species is largely unknown (8,9). A model for the interference was presented by Craig and Small (7) which accounts for much of the MSB observed in mixed crystal spectra of phenanthrene but the absence of SVL spectra and the presence of significant guest-host interactions precluded the making of statements as to its importance in other molecules.

In the present paper, we reanalyze the Condon/Herzberg-Teller interference mechanism and apply it to the spectra we have obtained for phenanthrene and phenanthrene-d_{10} in supersonic expansions of helium. Important to this study is the ability to reproduce band intensities observed in both photoexcitation and dispersed fluorescence by calculation of transition moments from simple first order equations. In addition, we attempt to account for contributions to transition asymmetries from other vibronically induced sources to obtain as complete a picture as possible for vibronic activity in a molecule which appears to present few extraneous complications.

EXPERIMENTAL

The rotationally cooled laser induced fluorescence (RC-LIF) apparatus used in this study is similar to that used previously (1), but several modifications have been made to improve sensitivity and reduce noise. A Quanta-Ray PSV-2 pulsed valve with a 0.5 mm orifice is used as the jet nozzle. Thermally equilibrated vapor pressures from solid samples at up to 110°C are obtained by placing the samples inside the heated valve assembly head of the PSV-2. Sample vapors are diluted with helium maintaining a constant total backing pressure of 1 to 10 atm.

The aluminum walled supersonic expansion chamber is evacuated by a 1740 L/s 6" diffusion pump stack which maintains an internal chamber pressure of 1-5 x 10^{-5} Torr during normal valve operation. The output of a Quanta-Ray Nd:YAG pumped dye laser ($\leq$0.4 cm^{-1} FWHM) is frequency doubled with a KDP crystal mounted in an Inrad Autotracker, and then lightly focused through light baffles into the expansion chamber where it intersects the rotationally cooled jet 1.0 cm downstream of the orifice. The laser beam is then exited from the chamber and directed into a solution of rhodamine B where the resulting fluorescence is detected with a photomultiplier tube, providing a reference for the laser intensity.

The light baffle arms used are made with polished homemade beam skimmers (10) and Brewster angle windows. This combination has allowed us to obtain jet spectra which are virtually free of scattered light contributions.

Fluorescence from the laser/jet interaction region is collected using f/1.0 optics mounted inside the chamber and focused onto the slits of either of two Instruments SA spectrophotometers. For dispersed fluorescence spectra, a 0.32 meter monochromator is used. For photoexcitation spectra, a 0.10 instrument is used. For these latter spectra, the holographic grating is typically used in zero order so that the spectrophotometer acts only to attenuate the collected fluorescence intensity. Under conditions where scattered light levels are appreciable, it is used in first order by centering its 160 Å bandpass red of the laser wavelength in a spectral region of strong phenanthrene fluorescence.

The outputs from the signal (Hamamatsu R106-UH) and reference (RCA 1P28) photomultiplier tubes are sent to a Quanta-Ray DGA-1 gated amplifier and ratioed. The normalized signal is then digitized and averaged by an LSI-11 based computer where the datum is stored for later analysis and display. Scanning of both the laser and monochromator wavelengths are computer controlled. For dispersed fluorescence spectra, a spectrum is obtained by collecting data while slewing the monochromator across the region of interest repetitively while simultaneously averaging the data. In this manner, day long scans can be recorded without distortions across the spectra due to long term baseline drifts and response changes. Relative intensities reported from these scans are, thus, accurate to within the approximation of a flat spectral response of the photomultiplier tube. Careful normalization to laser intensity further ensures accurate relative intensities (to within 5%) in photoexcitation spectra as well.

In some instances, the pressure tuned etalon option in the dye laser is utilized to obtain high resolution (0.05 cm^{-1} FWHM) excitation scans over short regions (~18 cm^{-1}) of the spectrum. The output voltage of a calibrated pressure transducer is then recorded simultaneously with the fluorescence intensity to determine relative band positions and contour widths.

Phenanthrene (Fluka, 97%) is used after 80-100 passes through a zone refiner. Phenanthrene-d_{10} (MSD Isotopes, 98.5%) is used without further purification. Photoexcitation spectra from samples of the latter reveal significant contributions from anthracene-d_{10}. However, spectra obtained by centering the 160 Å bandpass of the 0.10 meter monochromator at 3500 Å show no apparent contribution from the impurity as the latter displays only broadband fluorescence well red of the excitation wavelength in the spectral region of interest. To ensure accurate relative intensities for phenanthrene-d_{10} in photoexcitation, band intensities quoted or displayed are obtained from spectra using zero order detection.

RESULTS AND DISCUSSION

State Symmetries and Vibrational Mode Assignments

Phenanthrene possesses C_{2v} symmetry in both its ground ($^1A_1$) and first excited ($^1A_1$) singlet states. Though this system (11) is intrinsically weak in absorption (f=0.003), vibronic coupling with higher electronic states (12,13) allows for transitions involving the 22 planar modes of b_2 symmetry and the 10 out of plane modes of b_1 symmetry in addition to the 23 Condon allowed a_1 modes. [Here we have taken the z-axis as the axis of symmetry with y as the planar long axis of the molecule. This convention differs with that of ref. 14 and, thus, our reported symmetry designations also differ by interchange of b_1 and b_2.] Furthermore, the totally symmetric modes additionally derive Herzberg-Teller induced activity by coupling through S_3 ($^1A_1$) which lies at ~40,000 cm^{-1} and carries a significant oscillator strength (f=1.1). Modes of b_2 symmetry couple through S_2 ($^1B_2$ at 35375 cm^{-1}) which, though closer in resonance with S_1(29328 cm^{-1}), possesses a much lower oscillator strength (f=0.18).

In Table 1, we present a summary of our assignments of the planar vibrational modes of phenanthrene in the ground and first excited singlet states. Assignments are based on data summarized in this manuscript from photoexcitation spectra (both "low" resolution and rotationally resolved) and dispersed fluorescence spectra (both origin and vibronically excited). Results from pure (11) and mixed (12-15) crystal studies and from the normal coordinate analyses of Schettino et al. (14)

Table 1. Vibrational mode assignments for phenanthrene. Intensities observed in excitation and 0° fluorescence for $\Delta v = 1$ transitions are given in parentheses after the vibrational frequencies which are in cm^{-1}. WHS is from this work, F from ref. 15, HS from ref. 12, CG from ref. 11, and SNC from ref. 14. The bracketed frequencies from SNC are calculated values

	S_1				S_0		
#	WHS	F	HS	CG	WHS	HS	SNC
a_1 MODES:							
23	238 (7)	260 (<1)	237 (VVW)	218 (VW)	246 (3)	252 (M)	250
22	395 (0.3)	---	395 (S)	395 (M)	408 (21)	409 (VS)	406
21	517 (43)	520 (24)	523 (W)	516 (M)	544 (6)	549 (M)	540
20	673 (84)	676 (44)	674 (VS)	671 (S)	714 (12)	712 (MS)	710
19	817 (10)	819 (10)	811(VW)	---	833 (13)	828 (S)	830
18	1021 (8)	1027 (<1)	1028 (M)	1025 (W)	1043 (10)	1037 (S)	1038
17	1038 (3)	1074 (<1)	----	----	1065 (1)	1072 (W)	1100
16	----	----	----	----	----	----	1142
15	----	1110 (<1)	1126 (--)	1119 (VW)	1165 (1)	1181 (W)	1160
14	1207 (8)	----	1218 (VW)	1216 (VW)	1199 (2)	1206 (M)	1200
13	1246 (6)	----	1248 (WM)	1254 (W)	1257 (1)	----	1244
12	1337 (2)	1329 (<1)	1329 (M)	----	----	----	1303
11	1377 (57)	1380 (20)	1380 (VS)	1376 (VS)	1355 (40)	1352 (VVS)	1365
	1380 (25)						

Table 1. Continued

	S_1				S_0		
#	WHS	F	HS	CG	WHS	HS	SNC
a_1 MODES:							
10	1410 (18)	----	1409 (MS)	1407 (VS)	1423 (6)	----	1417
9	1430 (34)	1449 (2)	1441 (M)	1446 (S)	1450 (26)	1443 (VVS)	1441
8	1487 (9)	1485 (2)	1484 (W)	----	1526 (1)	----	1524
7	1529 (6)	1522 (2)	1519 (S)	1519 (s)	1580 (2)	1569 (--)	1567
6	1602 (13)	1599 (6)	----	1588 (W)	1613 (18)	1606 (VS)	1608
b_2 MODES:							
$\overline{22}$	429 (1)	404 (4)	436 (VVW)	---	471 (1)	---	[422]
$\overline{21}$	486 (6)	489 (2)	488 (VVW)	---	500 (1)	---	[469]
$\overline{20}$	591 (30)	591 (3)	583 (MS)	589 (W)	620 (12)	621 (VW)	618
$\overline{19}$	702 (32)	707 (21)	707 (MS)	699 (W)	731 (0)	---	[716]
$\overline{18}$	833 (13)	836 (9)	836 (MS)	---	875 (20)	865 (M)	[836]
$\overline{17}$	957 (5)	958 (1)	---	932 (VW)	---	---	1002
$\overline{16}$	1016 (6)	1015 (3)	1013 (WM)	1025 (W)	1019 (1)	----	1039
$\overline{15}$	----	----	----	----	----	----	[1095]

Table 1. Continued

	S_1				S_0		
#	WHS	F	HS	CG	WHS	HS	SNC
b_2 MODES:							
$\overline{14}$	----	----	----	----	----	----	1148
$\overline{13}$	----	1168 (<1)	1148 (W)	----	----	1181 (W)	1220
$\overline{12}$	----	1207 (8)	----	----	----	----	1303
$\overline{11}$	----	----	----	----	----	----	[1354]
$\overline{10}$	1373 (6)	1373 (5)	----	----	1434 (6)	----	1430
$\overline{9}$	1383 (21)	1389 (12)	----	----	----	----	1458
$\overline{8}$	----	1410 (14)	----	----	----	----	1500
$\overline{7}$	----	1429 (8)	1424 (M)	----	----	----	1548
$\overline{6}$	----	----	----	----	----	----	1670

are also presented. Ordering of modes is based on a standard scheme. Totally symmetric modes are numbered in decreasing order of frequency. Modes of b_2 symmetry are similarly ordered but are barred. Thus, for example, the lowest frequency b_2 mode is $\overline{22}$. Throughout this manuscript transitions between S_0 and S_1 involving changes in vibrational quanta in a given mode are denoted X_{ℓ}^{m} where the transition involves ℓ quanta of mode X in the ground state and m quanta in S_1. The appearance of a mode designation with only a superscript or only a subscript implies that we are referring to a vibronic state in S_1 or S_0, respectively, and not a transition.

It should be noted that the ten highest frequency planar vibrations (i.e., 1 through 5 and $\overline{1}$ through $\overline{5}$) are not included in Table 1. These modes, which lie $\gtrsim$2900 cm^{-1}, involve primarily C-H stretching motions and contribute little to the observed spectra. We have also neglected to include data concerning the ten b_1 and eleven a_2 modes. Though the former are formally vibronically allowed, we have no evidence that any of these nonplanar vibrations carry nonnegligible intensity in the $S_0 \rightleftarrows S_1$ system. [In fact, we do observe bands at 156 cm^{-1} in photexcitation and 148 cm^{-1} in 0^0-fluorescence which are likely assignable to transitions involving the 10 (b_2) "butterfly" vibration. These features are, however, extremely weak and positive identification is not possible. Our excitation spectra over the S_2 origin region shows a 90 cm^{-1} vibronic feature which is probably also due to an out of plane vibration.]

A compilation similar to Table 1 could be readily constructed for phenanthrene-d_{10}. But our results are incomplete by comparison and

since our interest in this species is focused on a few transitions, we omit it.

Excitation and Origin Excited Dispersed Fluorescence MSB

Portions of the photoexcitation and origin excited dispersed fluorescence spectra of phenanthrene are shown in Figs. 1 and 2, respectively. The bands are displayed relative to the 29328 cm^{-1} 0_0^0 transitions indicating vibrational frequencies in the S_1 and S_0 states, respectively. All of the observed features with intensities $\gtrsim$1% of the 0_0^0 bands are both temperature and pressure independent indicating that they are neither hot bands nor due to van der Waals species. Linewidths observed in excitation are ~1 cm^{-1} while in fluorescence they are instrument limited at 10 cm^{-1}. Portions of the origin excited dispersed fluorescence spectrum have been obtained using 5 cm^{-1} resolution. All of the bands observed in the spectra with intensities $\gtrsim$2% of the origin bands are assignable in terms of fundamentals and combinations of the vibrational modes listed in Table 1. Intensities of the fundamental transitions in these spectra are given in parentheses after the vibrational frequencies. Comparison of the tabulated intensity data with previous results reveals the need for medium-free conditions in analyzing intramolecular vibronic effects.

The most notable difference in the appearance of the spectra is in the intensities of the vibronic bands relative to the 0_0^0 bands. In excitation, several bands have intensities comparable to the origin transition while in fluorescence, this transition dominates the spectrum. This occurrence, in addition to the presence of drastic asymme-

Figure 1. Photoexcitation spectrum of phenanthrene. Band intensities are normalized to laser intensity. Band positions are displayed relative to the 29328 cm^{-1} origin transition. Sample temperature is 98°C. Helium backing pressure is 2 atm.

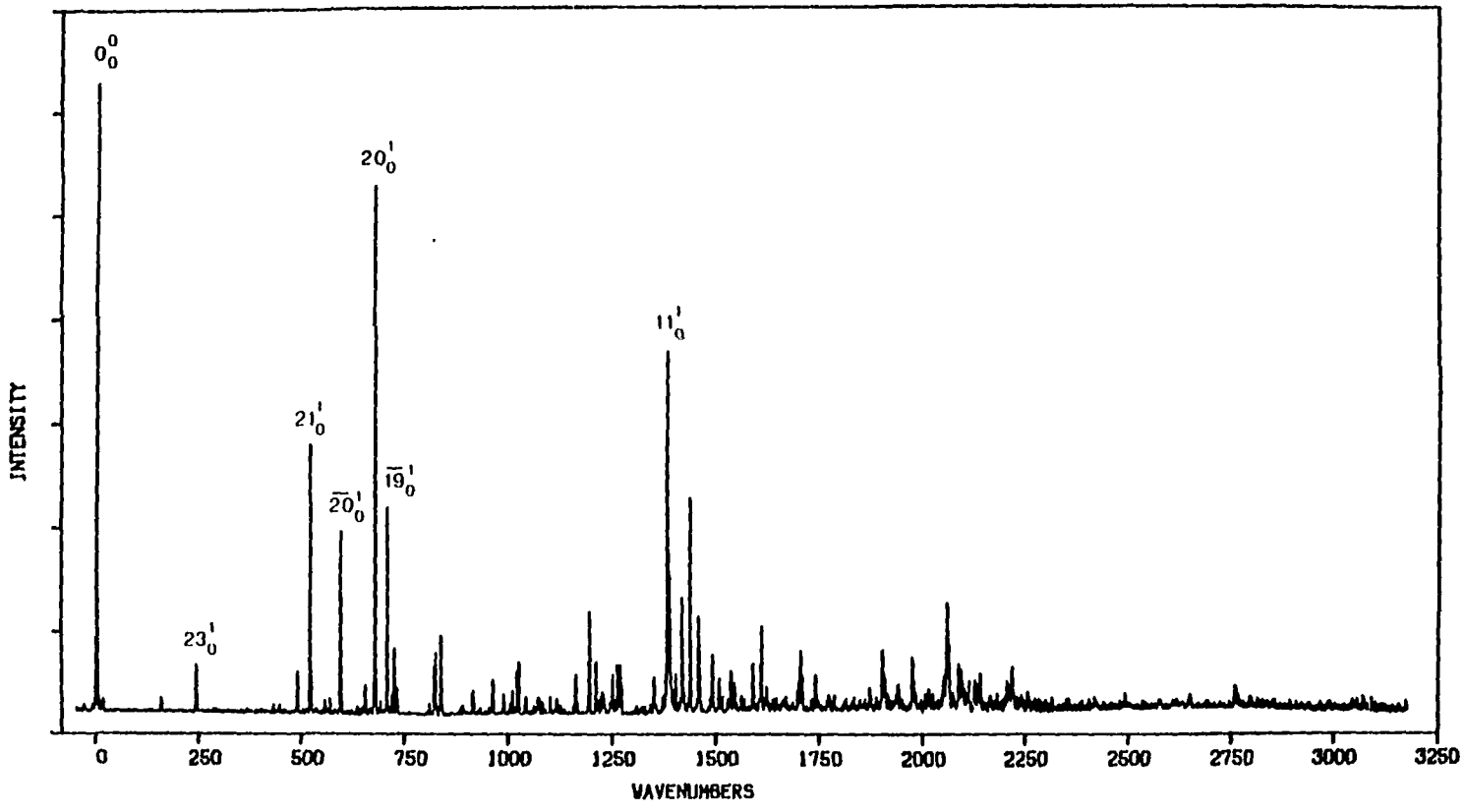
0_0^0
20_0^1
11_0^1
21_0^1
$\overline{19}_0^1$
$\overline{20}_0^1$
23_0^1
INTENSITY
0
250
500
750
1000
1250
1500
1750
2000
2250
2500
2750
3000
3250
WAVENUMBERS

Figure 2. Origin excited dispersed fluorescence spectrum of phenanthrene. Band positions are displayed relative to the 29328 cm^{-1} origin transition. Resolution is 10 cm^{-1}. T = 98°C. P_{He} = 2 atm.

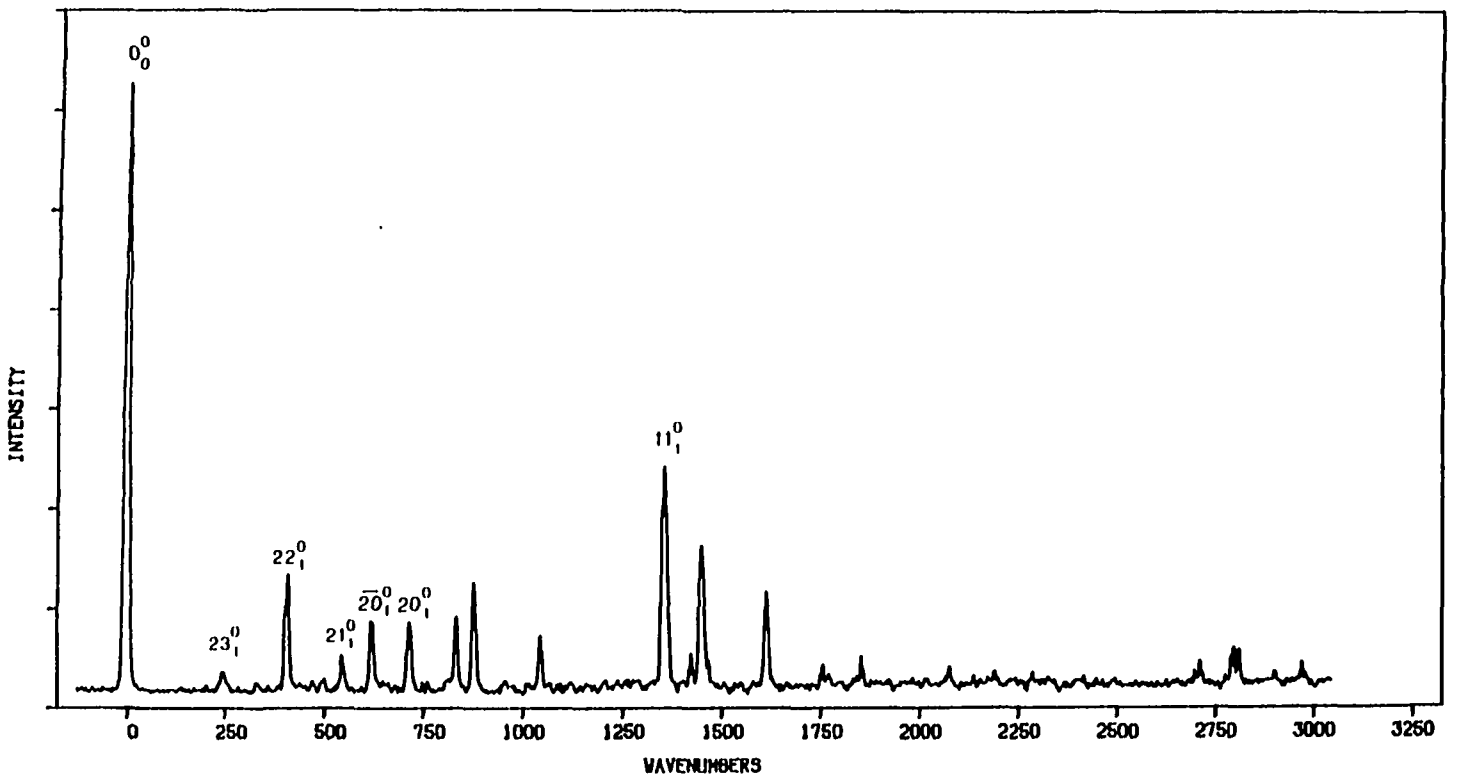
0_0^0
23_1^0
22_1^0
21_1^0
$\overline{20}_1^0$
20_1^0
11_1^0
INTENSITY
0
250
500
750
1000
1250
1500
1750
2000
2250
2500
2750
3000
3250
WAVENUMBERS

tries in the excitation and fluorescence intensities of a number of fundamental transitions, indicates that the source of MSB is vibronically induced and not simply the result of geometry changes experienced upon S_1 excitation. The presence of short progressions in both spectra involving mode 11 is the only evidence for a significant displacement of nuclear equilibrium positions in the two states involved. Similar progressions in planar ring "breathing" modes are commonly observed in linear polyacenes (e.g., benzene (16), naphthalene (17), and anthracene (18)) which show little or no MSB.

The degree of MSB displayed in the spectra of Figs. 1 and 2 is evidenced by the comparison of the intensities of X_0^1 transitions in absorption with their X_1^0 counterparts in fluorescence. These bands show intensity asymmetries which are quite substantial and vary from mode to mode with both the degree and the direction of asymmetry. The intensity of the 22_0^1 absorption, for example, is weaker than most identifiable hot bands in the spectrum and can only be identified by analogy with previous results and the absence of any other nearby features in the spectrum. In fluorescence, however, the 22_1^0 band is relatively intense. Several phenanthrene vibrations show similar behavior but with the absorption intensity enhanced over fluorescence. In still other modes, no asymmetry is observed.

Further examination of Table 1 reveals that while the excitation and fluorescence spectra between S_0 and S_1 differ markedly, the vibrational modes of the two states do not. Excitation into S_1 results in vibrational frequency defects ω_x'/ω_x of 0.94 to 0.98 while slight in-

creases in frequency are observed for modes 11 and 14. This latter effect is also common for the ring stretching vibrations in linear polyacenes (16-18). Such small frequency shifts support the observation of minimal coordinate displacement upon excitation into S_1.

Mode mixing, as a result of Fermi resonances or Duschinsky Rotation, does not appear to be important for phenanthrene in this system for a_1 bands below about 1300 cm^{-1}. Nearly all of the observed combination and overtone bands observed in excitation and fluorescence appear with vanishing (0 to 2 cm^{-1}) anharmonicities. Furthermore, the dispersed fluorescence spectra obtained by single vibronic level (SVL) excitation (via X_0^1) of a_1 vibronic bands below ~1300 cm^{-1} show single X_1^1 features of high "purity". For example, the SVL fluorescence spectrum obtained by excitation of the 20_0^1 transition shows the resonant 20_0^1 fluorescence band and a sharp transition readily assignable to 20_1^1 appears shifted 714 cm^{-1} to the red. This latter band acts as a false origin for 0°-like fluorescence which appears further to the red. Examination of the spectrum at our highest practical resolution shows no evidence of structure in the 20_1^1 fluorescence band. Such behavior is consistent with expectations based on similar or identical mode structures for the two electronic states. Finally, we note that only S_1 vibronic bands above 1300 cm^{-1} show the spectral broadening and congestion in SVL fluorescence indicative of the onset of intramolecular vibrational energy redistribution (IVER).

Absorption/fluorescence asymmetries in the intensities of the observed totally symmetric vibronic transitions are, thus, clearly not the

result of vibronic mode mixing, either static or dynamic, vibronically induced anharmonicity, or structural changes in the molecule. The absence of any known nearby electronic states would also seem to rule out any possible resonance interactions. Interference of Condon allowed and Herzberg-Teller induced transition moments for the totally symmetric vibronic levels does, however, appear to be operative. This effect, introduced heuristically by Sponer and Teller (19), was formalized by Craig and Small (7) to account for the MSB observed in the fundamental a_1 transitions of phenanthrene in mixed crystals. There, model calculations involving the varying of two parameters (the equilibrium coordinate displacement upon S_1 excitation and the Herzberg-Teller induced transition moment) for a given totally symmetric mode correctly predicted the intensities observed in absorption and fluorescence for a_1 bands. The lack of available data from low temperature crystal spectra concerning the weak $\Delta v > 2$ transitions (i.e., overtones) or $\Delta v = \pm 1$ transitions from hot band or SVL spectra essentially reduced the problem to the adjustment of two parameters to fit two data points. Though the final values used for the parameters were deemed reasonable based on other data, a test of the model to account for the intensities available from laser jet spectra would appear to be paramount. The absence of interfering effects, such as mode mixing, etc., clearly makes phenanthrene an ideal molecule for such a test.

In the next section, we review the formalism for this constructive/destructive interference and present results of model calculations

for transitions in phenanthrene and compare them to the intensity patterns observed.

Condon/Herzberg-Teller Transition Moment Interference

The electronic dipole transition moment between vibronic states gi and fj, where g and f are different adiabatic electronic states, can be written (20) as

$$\vec{M}_{gi,fj} = (i_g(Q)|\vec{M}_{gf}(Q)|j_f(Q)) \qquad (1)$$

where

$$\vec{M}_{gf}(Q) = \langle g(q,Q)|\vec{\mu}(q)|f(q,Q)\rangle \qquad (2)$$

and $\vec{\mu}$ is the electric dipole moment operator. The integrations performed in parentheses (|) are taken over the nuclear coordinates, Q, while those performed in brackets <|> are over the electronic coordinates, q.

We now perform the usual procedure of expansion of the electronic transition moment about the ground state equilibrium nuclear configuration, Q_o, in a Taylor series to obtain

$$\vec{M}_{gi,jf} = \vec{M}(Q_o)(i_g(Q)|j_f(Q)) + \sum_k \left(\frac{\partial \vec{M}(Q)}{\partial Q_k}\right)_{Q_o} (i_g(Q)|Q_k|j_f(Q))$$

$$+ \frac{1}{2} \sum_{k,l} \left(\frac{\partial^2 \vec{M}(Q)}{\partial Q_k \partial Q_l}\right)_{Q_o} \left(i_g(0)|Q_k Q_l|j_f(Q)\right) + \ldots \qquad (3)$$

where Q_k is the scalar displacement along the normal coordinate k measured from Q_o. For brevity's sake, we rewrite Eq. (3) as follows, retaining only the linear and zero order terms in Q_k:

$$\vec{M}_{gi,jf} = \vec{M}_o(i_g|j_f) + \sum_k \vec{m}_k(i_g|Q_k|j_f) \quad . \qquad (4)$$

At this point, it is important to note that the first term in Eq. (4), the Condon "allowed" moment, represents the electronic transition moment between adiabatic states originating from the nuclear configuration Q_o. Displacements of electronic state equilibria along Q_k are ignored in most treatments of vibronically induced moments since these usually concern transitions involving nontotally symmetric vibrations. In such cases, the Condon term vanishes and if the molecule of concern retains its point group symmetry upon excitation, there can be no equilibrium displacements along nontotally symmetric coordinates. However, for phenanthrene transitions involving a_1 vibrations, and for other molecules where totally symmetric vibrations contribute to the summation in Eq. (4), both terms must be retained. Furthermore, it is necessary to take into account the displacements of the fluorescing state origin along these coordinates from their equilibrium values in S_0.

From Eq. (4), we obtain for the absorption transition X_0^1 where mode X is totally symmetric,

$$\vec{M}_{X_0^1} = [\vec{M}_o(X^1|X_o) + \vec{m}_x(X^1|Q_x|X_o)]\prod_{k\neq x}(k^0|k_o) \qquad (5)$$

where we have assumed that the vibrational wavefunctions are products of simple harmonic oscillator functions and that only mode X carries Herzberg-Teller activity. In fluorescence, we now let the S_1 normal coordinate $Q_x' = Q_x + \delta_x$ where δ_x represents the equilibrium displacement along the coordinate. [Note that the sign convention for δ_x used here differs from that used in ref. 7. This results in a similar change in sign of the reported $\vec{m}_x/\vec{M}_o$ parameters.] Substitution into Eq. (4), thus, gives for the fluorescence transition

$$\vec{M}_{X_1^0} = [\vec{M}_o(X_1|X^0) - \vec{m}_x\delta_x(X_1|X^0) + \vec{m}_x(X_1|Q_x'|X^0)]\prod_{k\neq x}(k_o|k^0) \quad . \qquad (6)$$

For harmonic oscillators,

$$Q_x|X_v) = (\frac{v}{2\beta_x})^{1/2}|X_{v-1}) + (\frac{v+1}{2\beta_x})^{1/2}|X_{v+1}) \qquad (7)$$

where β_x is a constant. An identical relation holds for the excited state vibrational wavefunctions when Q_x and β_x are replaced by Q_x' and β_x'. Applying Eq. (7) and its counterpart to Eqs. (5) and (6) and drop-

ping the common product of 3N-5 Franck-Condon integrals, we obtain for the absorption transition

$$\vec{M}_{X_0^1} = \vec{M}_o(X^1|X_0) + \vec{m}_x\left(\frac{1}{2\beta_x}\right)^{1/2}(X^1|X_1) \qquad (8)$$

and for the corresponding fluorescence transition

$$\vec{M}_{X_1^0} = (\vec{M}_o - \vec{m}_x\delta_x)(X_1|X^0) + \vec{m}_x\left(\frac{1}{2\beta_x'}\right)^{1/2}(X_1|X^1) \quad . \qquad (9)$$

Calculations of the Franck-Condon integrals in Eqs. (8) and (9) are straightforward (21) and regarded as reliable for systems of harmonic oscillators having small displacements δ_x. It can be shown that for identical (or nearly so) vibrational frequencies ω_x and ω_x', the integral $(X_1|X^0) = -(X^1|X_0)$ while $(X^1|X_1) \equiv (X_1|X^1)$. [In all cases discussed, we have chosen $(X^1|X_0) > 0$ and report $|\delta_x|$ as δ_x.] Since the transition intensities for X_0^1 and X_1^0 are proportional to the squares of the moments given by Eqs. (8) and (9), respectively, it is clear that cross terms will be produced which will add or subtract with respect to the normal Condon and Herzberg-Teller contributions. Indeed, it can be seen that if constructive interference, leading to intensity enhancement, occurs in absorption, then destructive interference, leading to a loss of intensity, will occur in fluorescence and vice versa. The result is a loss of mirror symmetry in the absorption and fluorescence transition intensities for modes which are both Condon allowed and Herzberg-Teller

active. Equations for $\Delta v = 0, \pm 1, \pm 2, \ldots$ absorption and fluorescence transitions originating from any given vibronic state are readily obtained from Eqs. (5)-(7) with proper substitution of wavefunctions for the vibronic states involved. All transitions involving Herzberg-Teller active totally symmetric modes with nonzero Condon components will be similarly affected.

In Fig. 3, we graphically demonstrate the result of the interference represented in Eqs. (8) and (9). Intensities for $\Delta v = 1$ transitions (originating from the origins) in absorption and fluorescence (relative to the corresponding $\Delta v = 0$ transitions) are plotted for a vibration with $\omega_x = \omega_x' = 700\ cm^{-1}$ for displacements δ_x of 0 and 0.150 $amu^{1/2} a_0$. With the former condition, no asymmetry exists between absorption and fluorescence since the Condon allowed contributions vanish with zero Franck-Condon overlaps. However, with a small S_1 displacement, a large deviation from symmetry occurs for the transitions. It is important to note that where the intensity of one transition approaches zero, the change in the intensity of the weak transition with $\vec{m}_x$ is shallow. Thus, regions exist over wide ranges of $\vec{m}_x/\vec{M}_o$ which reflect near or total cancellation of transition intensity in either absorption or fluorescence. In such regions, MSB will be at a maximum and there will be "missing" bands in the spectrum. This behavior is consistent with observations made for phenanthrene.

In Table 2, we compare results of model calculations with the observed vibronic transition intensities involving the a_1 modes 20, 21, and 22 of phenanthrene. The calculated intensities presented were ob-

Figure 3. Calculated intensities for Condon/Herzberg-Teller interference. Plotted are the intensities, normalized to the $\Delta v = 0$ transitions, for the $\Delta v = 1$ absorption and fluorescence transitions originating from the origins for a totally symmetric mode X with $\omega_X = \omega'_X = 700\ cm^{-1}$. The dash-dotted line is for the two transitions calculated with $\delta_X = 0$. Solid lines are for absorption (lower left curve) and fluorescence (upper left curve) with $\delta_X = 0.15\ amu^{1/2}a_0$. Dashed curves are also plotted for the additional contribution of $\vec{m}_X^{BO}/\vec{M}_0 = 0.587\ amu^{-1/2}a_0^{-1}$ with $\delta_X = 0.15\ amu^{1/2}a_0$. $\vec{m}_X^{HT}/\vec{M}_0$ is in units of $amu^{-1/2}a_0^{-1}$

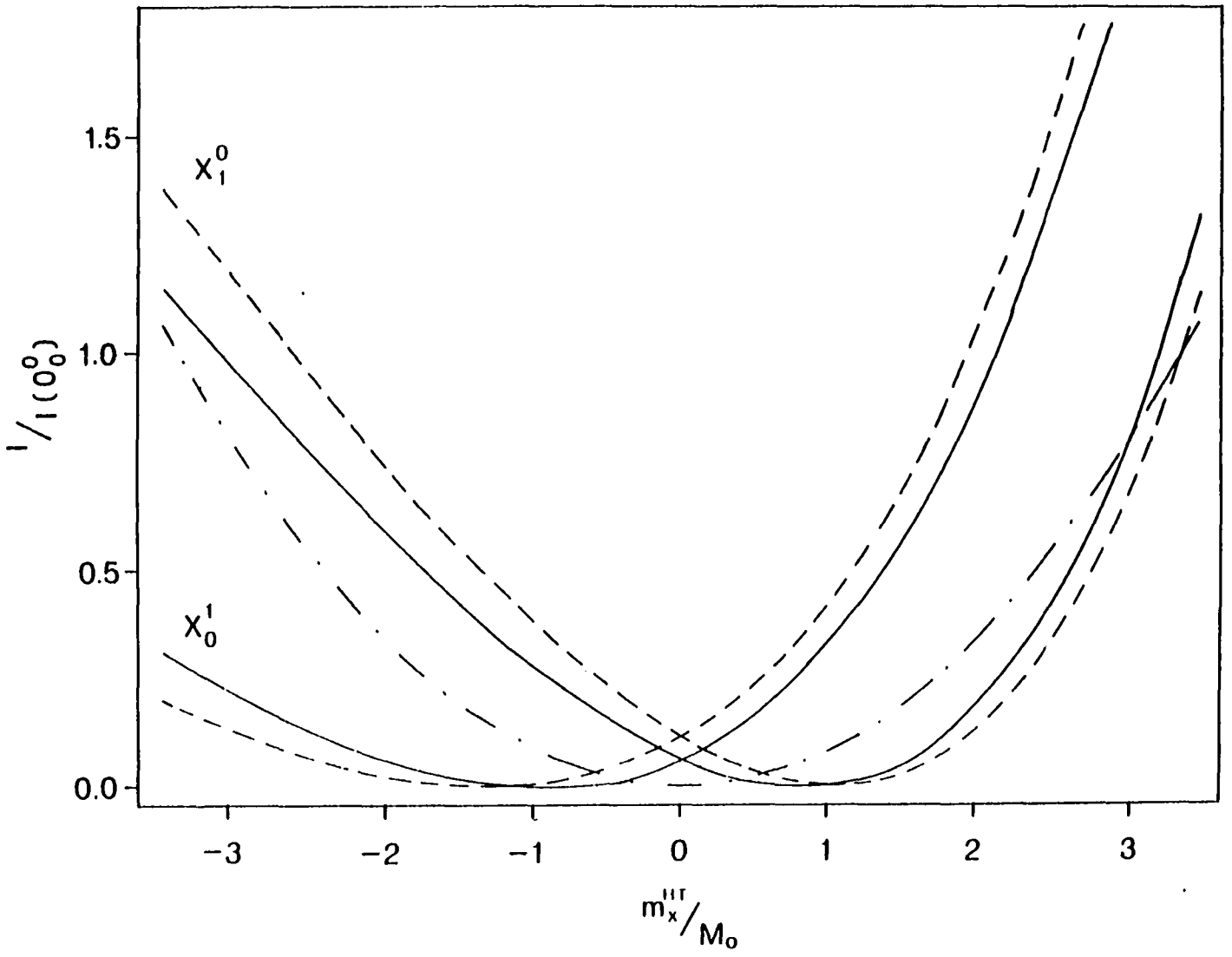
1.5
1.0
0.5
0.0
$I/I(0^o_o)$
X^0_1
X^1_0
−3
−2
−1
0
1
2
3
m'''_x/M_o

Table 2. Observed and calculated vibronic band intensities. Relative intensities for transitions originating from a given vibronic level are normalized to the $\Delta v = 0$ transition. Optimum parameter values used in the calculations are also given

		X = 20		X = 21		X = 22	
		Obs.	Calc.	Obs.	Calc.	Obs.	Calc.
Absorption:	X_0^0	100	100	100	100	100	100
	X_0^1	84	82	43	43	0.3	0.2
	X_0^2	7	8	1	2	0.2	0.2
Fluorescence:	X_0^0	100	100	100	100	100	100
	X_1^0	12	15	6	7	21	19
	X_2^0	<5	4	<1	1	1	1
	X_0^1	90	94	45	46	---	0.3
	X_1^1	100	100	100	100	---	100
	X_2^1	30	33	15	16	---	40
$\vec{m}_x/\vec{M}_o$ (amu$^{-1/2}$ a_0^{-1})		-1.91		1.26		-0.66	
δ_x (amu$^{1/2}$ a_0)		0.150		0.130		0.150	

tained from first order equations analogous to (5) and (6) by varying δ_x and $\vec{m}_x/\vec{M}_o$ and maximizing the fit to our experimental data. The optimum values of these parameters are also provided. We note that for each mode listed in Table 2, both the experimental and calculated intensities of $\Delta v > 3$ transitions are unobservable within our sensitivity. Hot band intensities in our excitation spectra are too weak to provide usable data. Finally, we have attempted to obtain SVL fluorescence spectra by excitation of X_0^2 bands, but the intensities of these transitions are also too weak to give reliable fluorescence information.

It is clear, nevertheless, that a strong correlation exists between the calculated results using the model presented and those obtained from our jet spectra. In most cases, as revealed in Table 2, the deviation of the calculated results from the observed data are less than our experimentally derived error limits. The optimum values of the parameters used are also entirely reasonable. For example, calculated vibronic matrix elements for mode 20 of phenanthrene (13) predict $|\vec{m}_{20}|/|\vec{M}_o| \equiv 2.0\ \text{amu}^{-1/2}a_0^{-1}$ which compares favorably with the value of 1.91 used in our calculations. The values of δ_x used correspond to displacements on the order of 0.02 Å for each carbon nucleus, also consistent with our observation of minor S_1 origin displacements.

In consideration of Eq. (3), one may be reluctant to ignore second and higher order contributions to the calculated transition moments. Unlike for typical transitions involving nontotally symmetric modes, where only terms of odd order in Q_k are nonzero, no terms in the expansion for a_1 modes will be identically zero. Indeed, even terms in-

volving $(X^1|Q_k|X_0)$ where $k \neq x$ will now contribute. The key to circumventing this problem is in the realization that for small values of δ_x and (nearly) identical S_1 and S_0 mode structures, all such terms will become negligible. To confirm this, we have performed intensity calculations similar to those presented in Table 2 but with the inclusion of terms to second order in Q and allowing for contributions involving $(X^1|Q_k|X_0)$ for $k \neq x$. The results from these calculations show that slight improvements in the correlated intensity patterns can be obtained, but only at the expense of "juggling" additional parameters to adjust the relative magnitude of terms which are intrinsically minor. It is obvious that, for phenanthrene at least, only calculations to first order in Q_x are necessary to model the data.

Finally, we note that while the model presented for MSB arising from Condon/Herzberg-Teller interference correctly predicts the intensity pattern observed for phenanthrene, it fails to account for changes observed upon perdeuteration of the molecule. Figures 4 and 5 show portions of the excitation and 0^0 dispersed fluorescence spectra obtained for phenanthrene-d_{10}. As in the case of phenanthrene, the observed transition frequencies agree well with previous results and bands are easily assigned. Again, MSB is observed (though to a lesser degree) in a number of transitions involving modes which are nearly identical in S_1 and S_0 and which show only minor deuteration shifts in frequency. No evidence for mode mixing is detectable from SVL spectra of low energy a_1 vibronic levels.

Figure 4. Photoexcitation spectrum of phenanthrene-d_{10}. Band intensities are normalized to laser intensity. Band positions are displayed relative to the 29421 cm^{-1} origin transition. Sample temperature is 95°C. Helium backing pressure is 2 atm. The 0_0^0 feature of impurity phenanthrene-h_{10} is also shown

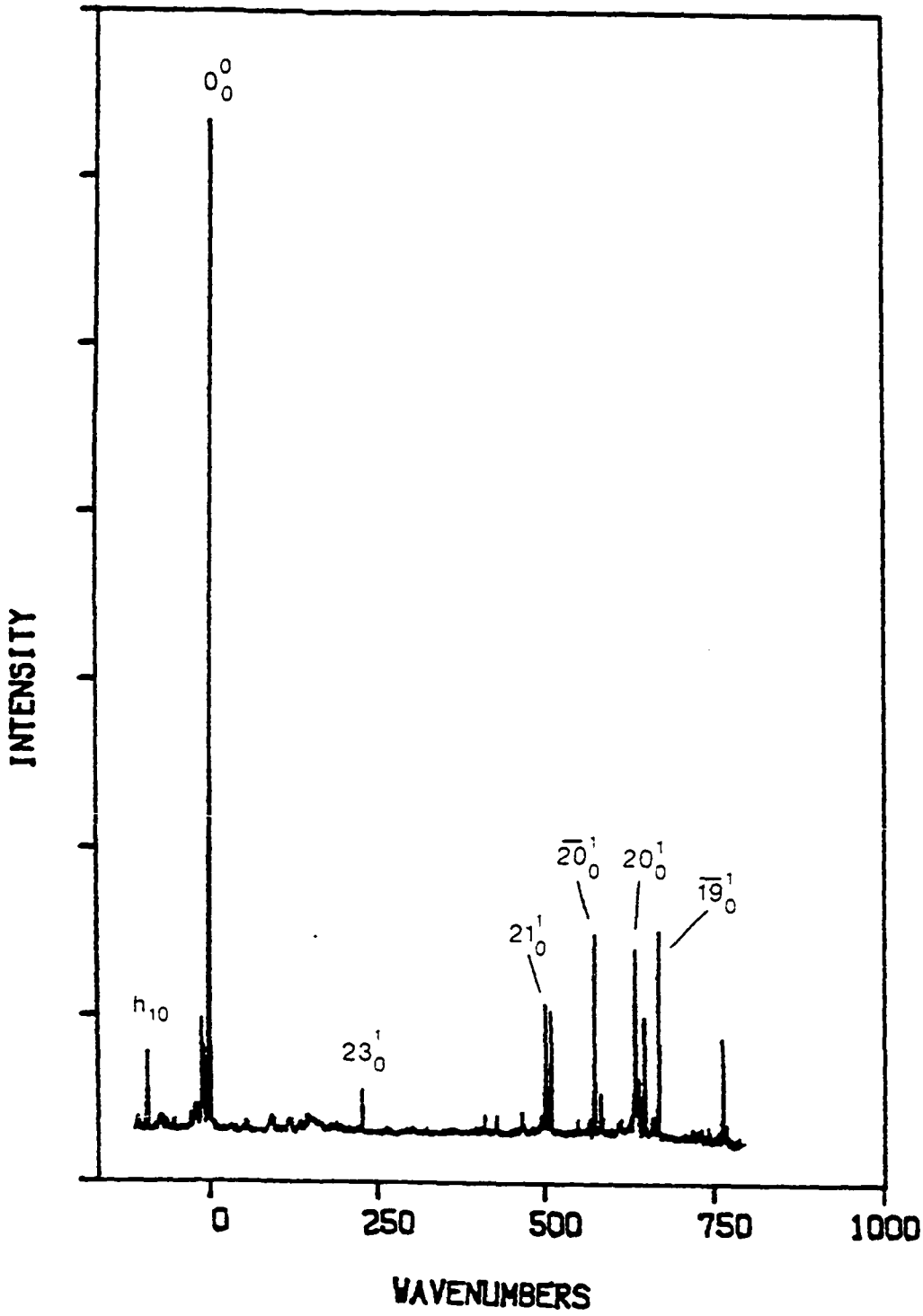
0_0^0
h_{10}
23_0^1
21_0^1
$\overline{20}_0^1$
20_0^1
$\overline{19}_0^1$
INTENSITY
0
250
500
750
1000
WAVENUMBERS

Figure 5. Origin excited dispersed fluorescence spectrum of phenanthrene-d_{10}. Band positions are displayed relative to the 29421 cm^{-1} origin transition. Resolution is 10 cm^{-1}. T = 95°C. P_{He} = 2 atm.

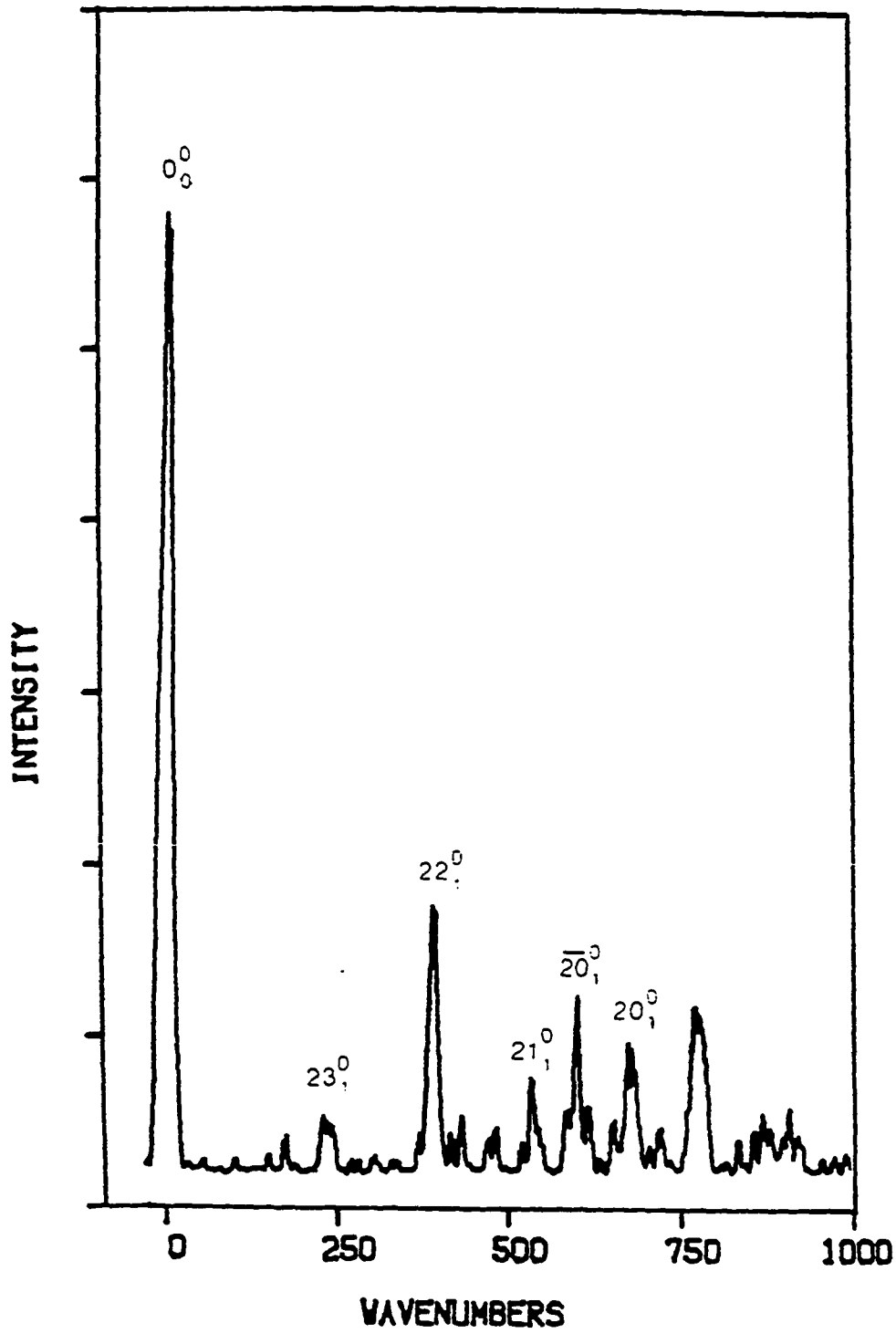
0_0^0
23_1^0
22_1^0
21_1^0
$\overline{20}_1^0$
20_1^0
INTENSITY
0
250
500
750
1000
WAVENUMBERS

By adjusting the parameters δ_x and $\vec{m}_x/\vec{M}_0$ for the mass of the per-deuterated species and making similar corrections to β_x and the Franck-Condon integrals, it is expected that the observed intensities for phenanthrene-d_{10} can be reproduced by calculation from the optimized parameters used for phenanthrene-h_{10}. However, the extreme reductions in the observed intensities of 20_0^1 and 21_0^1, for example, present major discrepancies with our calculations, even with the inclusion of second order terms. [We have even attempted to ascribe the intensity losses, unsuccessfully, to second order terms involving vibrations (unknown to us) that might experience severe (50%) frequency reductions upon deuteration.] Quite simply, with deuteration shifts $\omega_D/\omega_H \sim 0.94$, deuteration should result in intensity changes, compared with phenanthrene, of only a few percent for reasonably intense bands. In the case of the 20_0^1 absorption, however, the observed intensity is only one fourth that seen in phenanthrene-h_{10}, while the corresponding 20_1^0 band in fluorescence does not change. Only by radical (30 to 70%) adjustments to both δ_x and $\vec{m}_x/\vec{M}_0$ can the observed intensities be reasonably reproduced. The necessity for simultaneously adjusting both parameters appears to rule out the effect as being due to a simple reduction in vibronic coupling matrix elements with upper electronic states. Room temperature solution spectra of phenanthrene and phenanthrene-d_{10} show no differences in upper state structure as evidenced by absorption. Nor does isotopic dynamic mixing (22,23) seem to be important since concomitant increases in other photoexcitation band intensities do not occur. The potential energy distributions for the normal vibrations of the two species as

calculated by Schettino and co-workers similarly reveal only minor changes upon deuteration (14,24).

Large deuteration effects in vibronic transitions have been traditionally treated as the result of nonadiabatic vibronic coupling (25,26). The isotope dependence of the Born-Oppenheimer coupling intensity contribution is $(\omega_D/\omega_H)^3$ where it is only $(\omega_D/\omega_H)^1$ for Herzberg-Teller contributions. However, for $(\omega_D/\omega_H) = 0.94$, this can account for only a small fraction of the observed effect. Indeed, by replacing $\vec{m}_x$ with $(\vec{m}_x^{HT} + \vec{m}_x^{BO})$ in absorption and with $(\vec{m}_x^{HT} - \vec{m}_x^{BO})$ in fluorescence (see Fig. 3), calculated results for both phenanthrene and phenanthrene-d_{10} show poorer correlations with observed data as the importance of the Born-Oppenheimer terms are increased. Thus, despite the telling isotope effect, nonadiabatic effects appear to be negligible for a_1 transitions in both molecules.

We may be cautioned in our assumption that changes observed in photoexcitation reflect similar changes in the absorption process. [The intensity of the 20_0^1 band in phenanthrene-h_{10} by direct absorption reported by Amirav et al. (27) is considerably weaker than our value. However, the signal to noise in their spectrum makes quantitative statements based on their data impossible.] However, vapor phase measurements of the S_1 lifetimes of phenanthrene in several degrees of deuteration (28-30) indicate that the isotope dependence on fluorescence quantum yield is minimal even with excitation into vibronic bands well above the S_1 origin. It is, thus, unlikely that nonradiative decay could ac-

count for a factor of four change in the intensity of a band less than 700 cm^{-1} above the 0^0 level.

It is tempting as well to invoke "experimental error" in the form of poor normalization to laser intensity, for example, to account for the anomalous deuteration effect on photoexcitation intensities. By placing samples of phenanthrene and phenanthrene-d_{10} in the sample holder together and recording the resulting excitation spectrum, it is clear that even in the unlikely event that the reported intensities of vibronic bands relative to the origins are in error, the factor of four change in the intensity of the 20_0^1 band is nevertheless real.

S_1 Mode Mixing

Since Condon/Herzberg-Teller interference can only occur if totally symmetric modes are involved, we are unable to apply the presented model to explain the MSB which is evident in the b_2 modes of phenanthrene. Table 1 reveals that here, too, significant absorption/fluorescence asymmetries are present in phenanthrene. Note, for example, the total absence of $\overline{19}_1^0$ in the 0^0 excited fluorescence spectrum. Only from SVL fluorescence from $\overline{19}^1$ can the ground state vibration be assigned. Yet, assignment of the intense 702 cm^{-1} excited state feature as $\overline{19}_0^1$ is unquestionable based on the obvious b_2 type rotational contour and the supporting polarization data in mixed crystals. The SVL spectrum, however, shows multiple Condon allowed bands in the region of $\overline{19}_1^1$. One prominent feature can be assigned to fluorescence terminating in $\overline{20}_1$. Similar mode mixing is evident in the SVL spectrum (Fig. 6) from excitation of the vibronic band we label as $\overline{20}_0^1$. [Though mode mixing of the

Figure 6. SVL fluorescence spectrum from excitation of $\overline{20}_0^1$ in phenanthrene. Resolution is 15 cm^{-1}. T = 100°C. P_{He} = 3 atm.

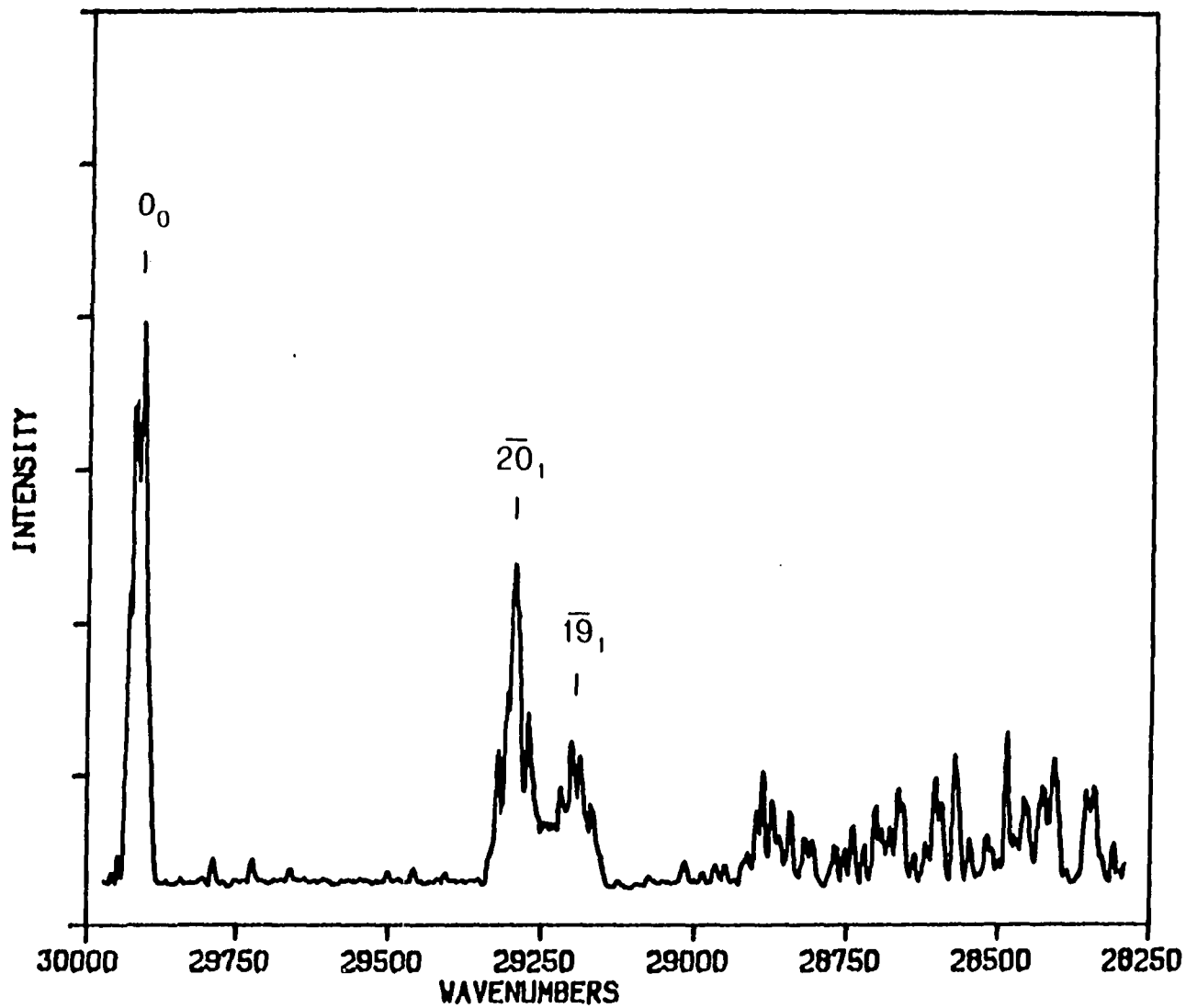
0_0
$\bar{2}0_1$
$\bar{1}9_1$
INTENSITY
30000
29750
29500
29250
29000
28750
28500
28250
WAVENUMBERS

b_2 vibronic levels in S_1 precludes the assignment of bands in excitation to pure ground state vibrations, we nevertheless assign these transitions based on the principal vibrational character displayed by each in SVL fluoresence.] Fluorescence transitions terminating in $\overline{20}_1$ and $\overline{19}_1$ are clearly present in the spectrum. It is, therefore, apparent that some mixing of S_1 vibronic levels occurs for at least some of the b_2 modes of phenanthrene. Since overtones and combinations of these bands appear in excitation with vanishing anharmonicities, we believe that the mixing is due to rotation of excited state normal coordinates (4-6) of b_2 symmetry relative to their S_0 coordinates resulting in MSB in absorption and fluorescence. It is interesting to note that a similar Duschinsky rotation of totally symmetric vibrations does not occur. We also note that as the lending state for vibronically induced intensity for b_2 vibrations lies only 6050 cm^{-1} above the S_1 origin, it is conceivable that nonadiabatic contributions to the spectral asymmetries may also be important. That is not the case for a_1 modes since the lending S_3 state lies to considerably higher energies.

Finally, we note that while mode mixing does not occur for a_1 vibrations below ~1300 cm^{-1}, some mixing is apparent from the SVL spectra obtained by excitation of S_1 bands near the 1380 cm^{-1} 11_0^1 transition. Because of the density of bands in this region of the excitation spectrum, we are not able to quantify the effect. Figure 7 displays a pressure tuned etalon scan over a portion of this region in excitation. At this wavelength, ~83 Torr N_2 corresponds to a 1 cm^{-1} scan in excitation. Contours are thus observed for vibronic bands at 1383, 1380, 1377, 1375,

Figure 7. Pressure tuned etalon excitation scan over the 1380 cm^{-1} S_1 region of phenanthrene. Excitation energy increases with decreasing N_2 pressure. 1 cm^{-1} corresponds to roughly 83 Torr. The strong doublet features in the center of the spectrum are part of a Fermi Resonance manifold which includes 11_0^1. Resolution is 0.05 cm^{-1}. T = 98°C. P_{He} = 2 atm.

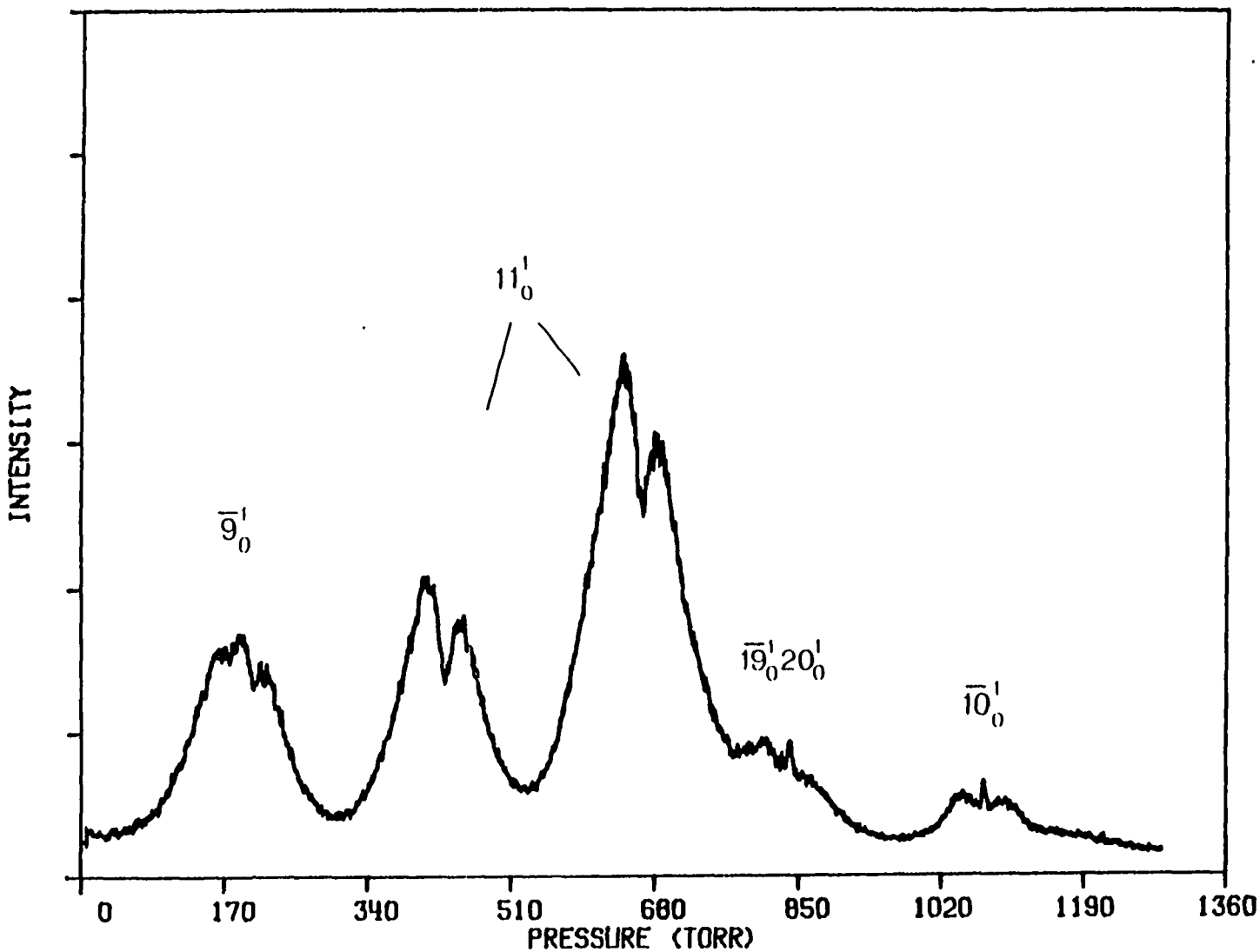
INTENSITY
11_0^1
$\bar{9}_0^1$
$\bar{1}9_0^1 20_0^1$
$\bar{1}0_0^1$
0
170
340
510
680
850
1020
1190
1360
PRESSURE (TORR)

and 1373 cm^{-1}. The appearance of a central Q-branch pileup in the contours of the 1383, 1375, and 1373 cm^{-1} bands clearly identify them as belonging to b_2 vibronic levels, namely $\overline{9}_0^1$, $\overline{19}_0^1 20_0^1$, and $\overline{10}_0^1$, respectively. The two most intense bands at 1380 and 1377 cm^{-1} lack this central feature, as does the 0_0^0 excitation band and are, thus, assignable to a_1 bands.

SVL fluorescence spectra obtained from excitation of several features in the region display significant spectral congestion. As a result, definitive assignments of some of the bands is not possible from our data and, for example, only the two most intense a_1 features are listed in the apparent resonance distorted spectrum corresponding to the carrying transition 11_0^1. Similar congestion as a result of Fermi resonance occurs in the 6_0^1 1380 cm^{-1}region of anthracene (18).

CONCLUSIONS

From the analysis of the spectra presented, several different contributions to the observed absorption/fluorescence MSB in phenanthrene can be delineated:

(1) Condon/Herzberg-Teller interference to first order in Q occurs in transitions involving totally symmetric vibrations. The interference is substantial for some modes, resulting in the total cancellation of intensity of one transition, while other modes display minimal interference effects.

(2) Mode mixing as a result of a Duschinsky rotation of S_1 normal coordinates occurs for modes of b_2 symmetry. It appears that some interference from Born-Oppenheimer induced moments may also occur for vibrations of this symmetry.

(3) Mode mixing as a result of Fermi resonance occurs for totally symmetric vibronic levels near 1380 cm^{-1} in S_1. Advanced mode mixing to higher energies is evident with the onset of IVER in this region.

(4) An isotope dependent contribution is present which cannot be accounted for by the above mechanisms.

REFERENCES

1. J. A. Warren, J. M. Hayes, and G. J. Small, J. Chem. Phys. 80 (1984) 1786.

2. J. A. Warren and G. J. Small, Chem. Phys., submitted.

3. See, for example, (a) A. R. Auty, A. C. Jones, and D. Phillips, Chem. Phys. Lett. 112 (1984) 529; (b) M. Fujii, T. Ebata, N. Mikami, M. Ito, Chem. Phys. 77 (1983) 191; (c) I. Y. Chan and M. Dauts, J. Chem. Phys. 82 (1985) 4771; (d) T. Ebata, Y. Suzuki, N. Mikami, T. Miyashi, and M. Ito, Chem. Phys. Lett. 110 (1984) 597; (e) J. Subbi, Chem. Phys. Lett. 109 (1984) 1; (f) D. Klapstein, R. Kuhn, J. P. Maier, M. Ochsner, and W. Zamback, J. Phys. Chem. 88 (1984) 5176; (g) A. Oikawa, H. Abe, N. Mikami, and M. Ito, J. Phys. Chem. 88 (1984) 5180.

4. F. Duschinsky, Acta Physicochim. 7 (1937) 551.

5. G. J. Small, J. Chem. Phys. 54 (1971) 3300.

6. B. Sharf and B. Honig, Chem. Phys. Lett. 7 (1970) 132.

7. D. P. Craig and G. J. Small, J. Chem. Phys. 50 (1969) 3827.

8. F. Fischer, S. Jakobson, and B. Scharf, Chem. Phys. 16 (1976) 237.

9. H. Shyldkrot and B. Scharf, Chem. Phys. 60 (1981) 249.

10. J. E. Butler, Appl. Opt. 21 (1982) 3617.

11. D. P. Craig and R. D. Gordon, Proc. Roy. Soc. (London) A288 (1965) 69.

12. R. M. Hochstrasser and G. J. Small, J. Chem. Phys. 45 (1966) 2270.

13. G. J. Small, Ph.D. Dissertation, University of Pennsylvania, Philadelphia, Pennsylvania, 1967.

14. V. Schettino, N. Neto, and S. Califano, J. Chem. Phys. 44 (1966) 2724.

15. G. Fischer, Chem. Phys. 4 (1974) 62.

16. P. Langridge-Smith, D. Brumbaugh, C. Hyaman, and D. H. Levy, J. Phys. Chem. 85 (1981) 3742.

17. S. M. Beck, J. B. Hopkins, D. E. Powers, and R. E. Smalley, J. Chem. Phys. 74 (1981) 43.

18. W. R. Lambert, P. M. Felker, J. A. Syage, and A. H. Zewail, J. Chem. Phys. 81 (1984) 2195.

19. H. Sponer and E. Teller, Rev. Mod. Phys. 13 (1941) 75.

20. G. Fischer, In Vibronic Coupling (Academic Press, London, 1984).

21. J. R. Henderson, M. Muramoto, and R. A. Willett, J. Chem. Phys. 41 (1964) 580.

22. G. Orr and G. J. Small, Chem. Phys. Lett. 21 (1973) 395.

23. G. Orr and G. J. Small, Chem. Phys. 2 (1973) 60.

24. V. Schettino, J. Chem. Phys. 46 (1967) 302.

25. G. Orlandi and W. Siebrand, Chem. Phys. Lett. 15 (1972) 465.

26. G. Orlandi and W. Siebrand, J. Chem. Phys. 58 (1973) 4513.

27. A. Amirav, M. Sonnenschein, and J. Jortner, J. Phys. Chem. 88 (1984) 5593.

28. A. E. W. Knight and B. K. Selinger, Aust. J. Chem. 26 (1973) 499.

29. J. J. O'Brien, B. R. Henry, and B. K. Selinger, Chem. Phys. Lett. 46 (1977) 271.

30. J. J. O'Brien, M. D. Horne, B. K. Selinger, B. R. Henry, Chem. Phys. 68 (1982) 123.

APPENDIX. ROTATIONALLY COOLED LASER INDUCED FLUORESCENCE DETERMINATION OF POLYCYCLIC AROMATIC HYDROCARBONS

INTRODUCTION

In recent years, the development of new highly selective and sensitive methods for the characterization and determination of polycyclic aromatic hydrocarbons (PAHs) and their derivatives in complex mixtures has received considerable attention. High selectivity is associated here with the ability to distinguish between substitutional isomers of PAHs. Attainment of this selectivity with capillary column-gas chromatography-mass spectrometry for complex mixtures is very difficult and time consuming. Alternative approaches are, therefore, required.

Given that the majority of PAHs fluoresce with reasonable quantum yields and that high sensitivities are afforded by fluorescence detection, the possibility of developing high resolution fluorescence based techniques is attractive. This is all the more so if the technique's selectivity does not rely on physical separation, e.g., chromatography. In this paper, discussion is limited to such techniques. They must, therefore, afford fluorescence vibronic bandwidths of only a few cm^{-1}. When low temperature solids are employed as host matrices for PAHs or other analytes of interest, the most general approach to achieving such linewidths is laser excited fluorescence line narrowing (1-10).

Given that fluorescence line narrowing spectrometry affords quasi-line fluorescence spectra for PAHs (as well as other species, e.g., rare earth ions (11)), its selectivity will often be limited by the vibronic absorption bandwidths of the PAHs. When organic glasses are employed these bandwidths are typically $\approx$300 cm^{-1} and are site inhomogeneously

broadened. For Shpol'skii or rare gas matrices, the bandwidths can approach ~100 cm^{-1}. In this paper, we present data and discussion which show that rotationally cooled laser induced fluorescence (RC-LIF), a gas phase technique, possesses a selectivity which is significantly superior to the solid state methods discussed above. The enhanced selectivity results from the fact that absorption bands of rotationally cooled molecules seeded in supersonic jets (12) exhibit widths of about 1 cm^{-1}.

The availability of detailed spectroscopic information of rotationally cooled species under the collision-free conditions of these supersonic beams has led to a number of applications of RC-LIF (13). Molecules as large as ovalene (14) and free-base phthalocyanin (15-18) have been observed to exhibit absorption (obtained by photoexcitation) and emission spectra with linewidths which are typically instrument limited and with only minor contributions from vibrational hot bands. It, therefore, seems reasonable to expect that RC-LIF can be of use in the analysis of complex mixtures of large organic molecules (6).

In the present work, we report our observations of the photoexcitation and dispersed fluorescence spectra of naphthalene and the α and β isomers of methylnaphthalene from pure and mixed samples in a seeded supersonic expansion of helium. The ability to distinguish between these spectroscopically similar PAHs, in particular the geometric isomers of methylnaphthalene, provides a test of the usefulness of this technique in supplying information suitable for analytical determinations. The present limitations of the technique are also discussed.

EXPERIMENTAL

A diagram of the RC-LIF scheme is shown in Fig. 1. The output from a Quanta-Ray Nd:YAG pumped dye laser is frequency doubled by a KDP crystal mounted in an Inrad Autotracker. The doubled output is focused into the supersonic expansion chamber where it crosses the rotationally cooled beam. Light baffles are mounted along the laser entrance and exit arms of the chamber to reduce scattered light. The exiting laser beam is then deflected into a solution of rhodamine B where the resulting fluorescence is detected with a phototube, providing a reference for the laser intensity.

The supersonic expansion chamber is similar in design to that described elsewhere (13). The chamber was fabricated from 4-inch stainless steel tubing. Internal pressures of 0.1-5 mtorr are maintained during operation by two 4-inch oil diffusion pumps operating at 300 Ls^{-1} with a 50 Ls^{-1} mechanical forepump. The nozzle was made by heating an open end of 8 mm Pyrex tubing in a flame until a bulb with a pinhole was formed. The excess glass was then ground away leaving an orifice with a diameter of 160 ± 10 μm.

The focused laser beam intercepts the rotationally cooled beam 5 mm (~30 nozzle diameters) downstream of the orifice. The resulting fluorescence propagating perpendicular to the two beams is collected through a 2-inch quartz window and imaged onto the slits of a 0.32 m Instruments SA spectrometer where it is dispersed. The outputs from the signal and reference phototubes (both RCA 1P28-A) are sent to a pair

Figure 1. Diagram of the RC-LIF scheme

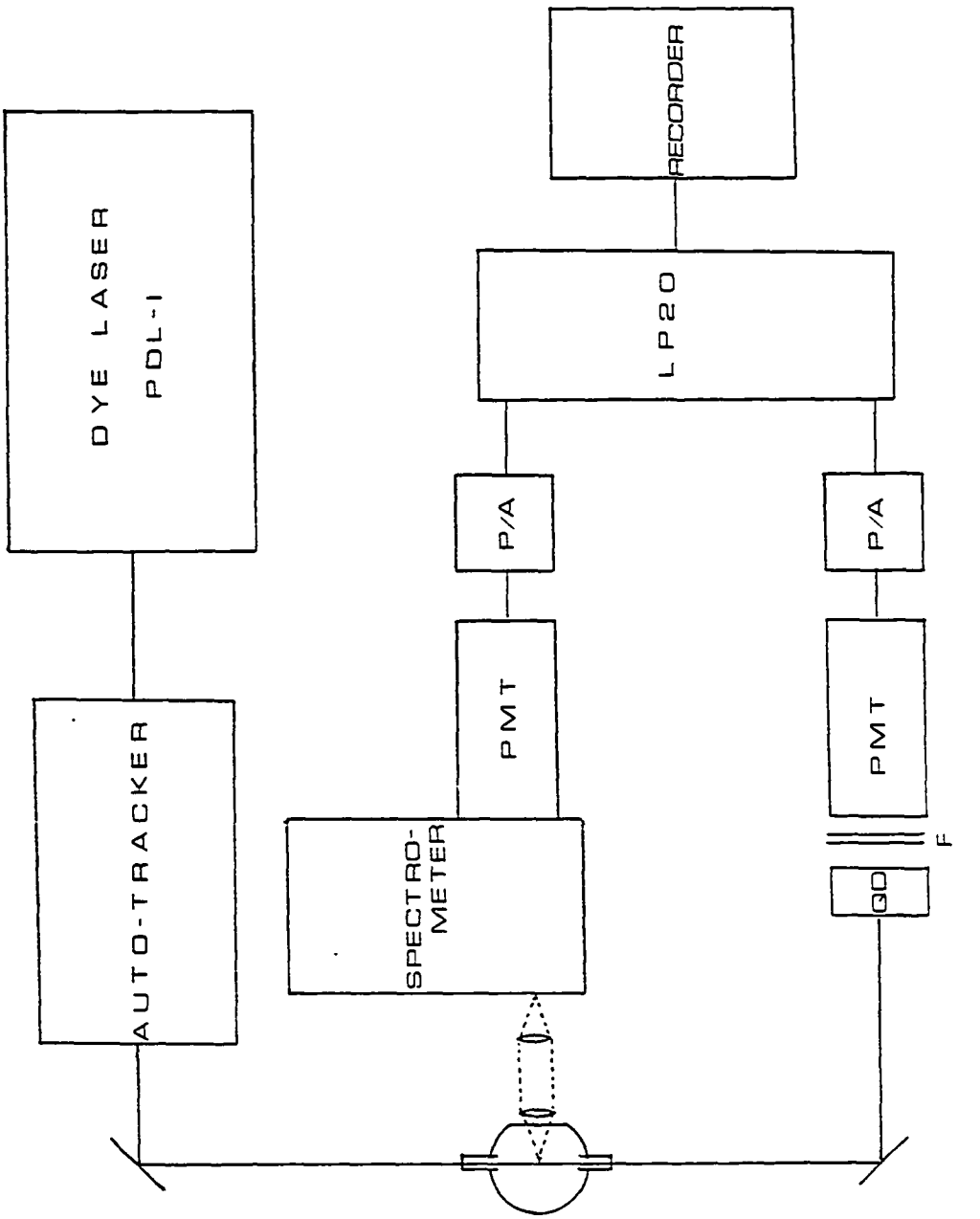
DYE LASER
PDL-1
AUTO-TRACKER
SPECTRO-
METER
PMT
P/A
LP20
RECORDER
P/A
PMT
QD
F

of charge sensitive, integrating preamplifiers and then to a Molectron LP-20 laser photometer, which averages the outputs separately. The outputs are then ratioed and sent to a strip chart recorder to record the normalized spectrum.

Samples were prepared from naphthalene (Aldrich, 98%), α-methylnaphthalene (Aldrich, 97%), and β-methylnaphthalene (Fluka, 97%) without further purification. The room temperature vapor pressure of the samples were diluted with He, maintaining a constant total pressure of 1.0-2.0 atm.

RESULTS AND DISCUSSION

A portion of the photoexcitation spectrum obtained from a mixture of naphthalene, α-methylnaphthalene, and β-methylnaphthalene is shown in Fig. 2. The sample consisted of an equimolar liquid mixture of α- and β-methylnaphthalene and a neat sample of solid naphthalene. On the basis of similar RC-LIF spectra obtained from pure samples, and from previous investigations (6,19), the features in the spectrum can be readily identified. With the exception of the weak, pressure sensitive hot band structure which appears at the low excitation energy side of the major bands, all of the bands in the spectrum can be directly assigned to transitions originating from the vibrationless level of the ground states to specific vibronic levels in the S_1 states of the three species. Specifically, the features occurring at 31,702 cm^{-1}, 31,772 cm^{-1}, and 32,020 cm^{-1} were identified as the S_1 origins of β-methylnaphthalene, α-methylnaphthalene, and naphthalene, respectively. Indeed, the spectrum appears directly as a weighted sum of the photoexcitation spectra from pure samples of the three constituents, showing no component interactions. No evidence of the formation of van der Waals molecules or polymers was observed (12,13). The absence of saturation broadening and other nonlinear laser intensity phenomena was confirmed by rerunning this and other spectra at reduced laser powers, with no observable changes.

In Fig. 2, the linewidths are laser limited (laser bandwidth ≅2 cm^{-1}). Previously (6), using a laser bandwidth of 0.7 cm^{-1}, we deter-

Figure 2. RC-LIF photoexcitation spectrum from a mixed sample of naphthalene, α-methylnaphthalene, and β-methylnaphthalene. N[0°], α[0°], and β[0°] denote their S_1 origin bands, respectively. Monitoring wavelength = 3425 A. Bandpass = 50 A

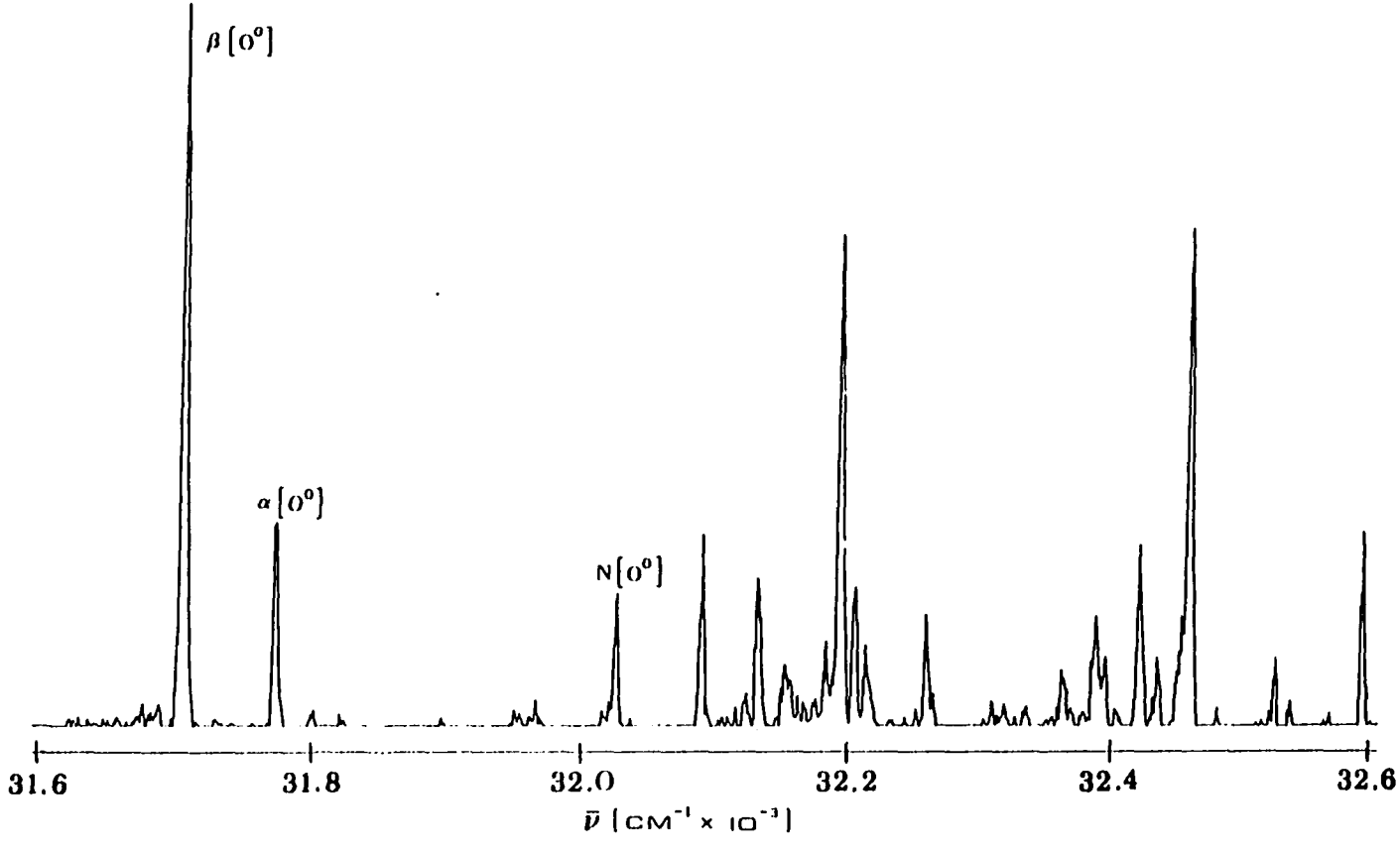
β [0°]
α [0°]
N [0°]
31.6
31.8
32.0
32.2
32.4
32.6
$\bar{\nu}$ [CM^{-1} x 10^{-3}]

mined that the width of the $\bar{8}^1$ band of naphthalene, occurring at 32,458 cm^{-1}, is still laser limited although some structure is resolvable. Such linewidths are typical, even at these low carrier gas pressures. Thus, Fig. 2 represents a relatively low resolution photoexcitation spectrum. Despite this, the bands in the spectrum are well resolved and allow for easy identification of the three components of the sample.

The identification of impurities in "pure" samples can be attained in this manner. In photoexcitation spectra of fresh samples of naphthalene, we have observed bands attributable to β-methylnaphthalene, indicating its presence as an impurity. Over a period of ~7 hrs. of operation, these bands disappear apparently due to degassing of the more volatile β-methylnaphthalene from the sample. In other samples, for instance, β-methylnaphthalene was doped with ~250 ppm naphthalene. Photoexcitation spectra of such samples clearly show the presence of the dopant.

The presence of impurities can also be determined from fluorescence spectra. Figure 3 shows the dispersed fluorescence spectrum from excitation of the 32,458 cm^{-1} $\bar{8}_0^1$ band of naphthalene. This spectrum is unchanged whether obtained from pure naphthalene or from a trace amount of naphthalene in β-methylnaphthalene. If this spectrum represented an unknown impurity in β-methylnaphthalene, it could be identified as such because it is impossible to interpret the spectrum in terms of β-methylnaphthalene vibrations. Together with the photoexcitation spectrum of the sample, an unambiguous identification of the impurity can be made.

Figure 3. Dispersed fluorescence spectrum by excitation of the $\bar{8}^1$ band (32458 cm^{-1}) of naphthalene. Instrument resolution = 1.25 A

FLUORESCENCE INTENSITY
310
330
350
λ [NM]

The data presented show that even in the photoexcitation mode rotationally cooled spectrometry of a simple mixture can readily distinguish between substitutional isomers of PAHs. This will usually not be possible with solid state techniques. Based on the linewidths in Fig. 2 and the earlier discussion of inhomogeneously broadened vibronic bandwidths of PAHs imbedded in solids, it is clear that the selectivity of RC-LIF is significantly superior (ten- to one hundred-fold) to that of fluorescence line narrowing spectrometry in organic glasses (4-6) or laser excited Shpol'skii spectrometry (9,10). We hasten to point out, however, that the selectivity of the latter two techniques is high and has allowed for the direct analysis of nonpolar PAHs in real samples (5,9). Recent work on polar derivatives of PAHs, e.g., amino-PAHs, has shown, however, that application of solid state fluorescence techniques presents difficulties due to strong analyte-matrix interactions (20). This suggests that RC-LIF spectrometry will be important for the characterization of species prone to strong matrix interactions which obviate fluorescence line narrowing spectrometry.

In assessing the analytical utility of RC-LIF spectrometry, its superior selectivity, adequate sensitivity and absence of matrix effects must be weighed against the fact that quantitation presents a serious problem for real samples. We are now initiating studies to determine whether RC-LIF, as a stand alone technique, can be made semiquantitative. For RC-LIF to be quantitative, it will be necessary to couple it with gas chromatography as has been discussed in earlier work (6).

REFERENCES

1. R. I. Personov, E. I. Al'Shits, and L. A. Bykovskaya, Opt. Commun. 6 (1972) 169.

2. A. Szabo, Phys. Rev. Lett. 25 (1970) 924.

3. A. Szabo, Phys. Rev. Lett. 27 (1971) 323.

4. J. C. Brown, M. C. Edelson, and G. J. Small, Anal. Chem. 50 (1978) 1394.

5. J. C. Brown, J. A. Duncanson, and G. J. Small, Anal. Chem. 52 (1980) 1711.

6. J. C. Brown, J. M. Hayes, J. A. Warren, and G. J. Small, In Lasers in Chemical Analysis, G. M. Hieftje, F. E. Lytle, and J. C. Travis, Eds. (Humana Press, Clifton, NJ, 1981), Chapter 12.

7. L. A. Bykovskaya, R. I. Personov, and Y. V. Romanovskii, Anal. Chim. Acta 125 (1981) 1.

8. E. V. Shpolskii, and T. N. Bolotnikova, Pure Appl. Chem. 37 (1974) 183.

9. Y. Yang, A. P. D'Silva, V. A. Fassel, and M. Iles, Anal. Chem. 52 (1980) 1350.

10. Y. Yang, A. P. D'Silva, and V. A. Fassel, Anal. Chem. 53 (1981) 894.

11. F. J. Gustafson, and J. C. Wright, Anal. Chem. 51 (1979) 1762.

12. D. H. Levy, L. Wharton, and R. E. Smalley, In Chemical and Biochemical Applications of Lasers, Vol. 2 (Academic Press, New York, 1977), Chapter 1.

13. R. E. Smalley, D. H. Levy, and L. Wharton, J. Chem. Phys. 64 (1976) 3266; and references therein.

14. A. Amirav, U. Even, and J. Jortner, Chem. Phys. Lett. 69 (1980) 14.

15. P. H. S. Fitch, L. Wharton, and D. H. Levy, J. Chem. Phys. 69 (1978) 3246.

16. P. H. S. Fitch, L. Wharton, and D. H. Levy, J. Chem. Phys. 70 (1979) 2018.

17. P. H. S. Fitch, C. Haynam, and D. H. Levy, J. Chem. Phys. 73 (1980) 1064.

18. P. H. S. Fitch, C. Haynam, and D. H. Levy, J. Chem. Phys. 74 6612.

19. M. Stockburger, H. Gatterman, and W. Klusman, J. Chem. Phys. 63 (1975) 4529.

20. I. Chiang, M.S. Thesis, Iowa State University, Ames, Iowa, 1981.

SUMMARY

From the data presented, it is clear that the application of laser jet spectroscopy to the study of vibronic activity in polyatomic molecules is a vital one. The ability to obtain excitation and unrelaxed fluorescence spectra of species in the absence of a perturbing medium greatly simplifies the problem of probing vibronic effects which are otherwise negligible or masked by interfering effects. Data obtained using the technique in studies of β-methylnaphthalene and phenanthrene have shown that the use of simple first order corrections to vibronic wavefunctions and transition moments can account for the vast majority of the structure observed in such spectra. Other effects arising from vibronic coupling will likely be amenable to analysis by laser jet spectroscopy. The anomalous isotope effect observed in the spectra of perdeuterated phenanthrene is, for example, an effect which will likely be explained from the analysis of laser jet spectra of various substituted phenanthrenes.

REFERENCES

1. J. A. Warren, J. M. Hayes, and G. J. Small, J. Chem. Phys. 80 (1984) 1786.

2. J. A. Warren, J. M. Hayes, and G. J. Small, Chem. Phys., submitted.

3. J. A. Warren, J. M. Hayes, and G. J. Small, Chem. Phys., submitted.

4. J. A. Warren, J. M. Hayes, and G. J. Small, Anal. Chem. 54 (1982) 138.

5. R. E. Smalley, D. H. Levy, and L. Wharton, J. Chem. Phys. 64 (1976) 3266 and references therein.

6. R. E. Smalley, B. L. Ramakrishna, D. H. Levy, and L. Wharton, J. Chem. Phys. 61 (1974) 4363.

7. J. E. Butler, Appl. Opt. 21 (1982) 3617.

ACKNOWLEDGEMENTS

I would here like to offer my thanks to a number of souls whose assistance throughout my years in college and graduate school have been invaluable. Uppermost among those who have spurred my interest in the details of molecular spectroscopy and dynamics is Professor Gerald J. Small. His clear insight in the field and his helpful discussions were often the only reason why the explanations for several interesting effects described in this manuscript were pursued.

Two permanent staff members, George R. Smith at the University of Utah and John M. Hayes at Iowa State University, have been of most importance in my development as an experimentalist.

Several graduate and undergraduate students with whom I have studied have been of great assistance in the development of this dissertation. Most notable among these is Bryan L. Fearey whose discussions with me often helped me to rethink solutions to problems with a different perspective.

I would like to thank Iowa State University and the Ames Laboratory. The research related here was supported by the U. S. Department of Energy through the Office of Basic Energy Sciences and the Office of Health and Environmental Research.

I would also like to thank my parents for their moral and financial support throughout my education.

Lastly, I would like to thank my wife, Jerri, for the encouragement and emotional support which she provided in the final stages of the

preparation of this thesis. Without her, this manuscript would likely not have been completed.